附件一

行政院國家科學委員會補助專題研究計畫 □ 成 果 報 告 ☑期中進度報告

操控半導體電子自旋的動力行為與傳輸的研究

計畫類別：☑ 個別型計畫　　□ 整合型計畫
計畫編號：NSC 96 － 2112 － M009 － 0038 －　MY3 －
執行期間：　2003 年 08 月　01 日至　2004 年 07 月 31 日

計畫主持人：朱仲夏 教授
共同主持人：
計畫參與人員：王律堯, 陳志高, 張榮興, 江吉偉, 邱志宣, 周昆宜, 吳智偉, 杜冠誼

成果報告類型(依經費核定清單規定繳交)：☑精簡報告　□完整報告

本成果報告包括以下應繳交之附件：
□赴國外出差或研習心得報告一份
□赴大陸地區出差或研習心得報告一份
■出席國際學術會議心得報告及發表之論文各一份
□國際合作研究計畫國外研究報告書一份

處理方式：除產學合作研究計畫、提升產業技術及人才培育研究計畫、列管計畫及下列情形者外，得立即公開查詢
□涉及專利或其他智慧財產權，□一年□二年後可公開查詢

執行單位：國立交通大學電子物理系

中　華　民　國　97　年　05　月　31　日

行政院國家科學委員會專題研究計劃成果報告

操控半導體電子自旋的動力行為與傳輸的研究:
(一)競爭性 Rashba 和 cubic-k Dresselhaus 本質自旋軌道交互作用對於產生自旋霍爾效應之影響探討；
(二)內稟自旋霍爾效應在低磁場下的不對稱性；
(三)自旋流之電性偵測；
(四)在 Rashba-type 二維電子氣中，由非均勻場所產生之自旋堆積；
(五)兩接頭的介觀環的 Fano 共振傳輸的研究，
(六)二維 cubic-k Dresselhaus-type 電子系統中 在圓盤附近的量子散射。

The manipulation of electron spin dynamics and transport in the semiconductor:
[I] Competing interplay between Rashba and cubic-k Dresselhaus spin-orbit interactions in spin-Hall effect ;
[II] Asymmetries in intrinsic spin-Hall effect in low in-plane magnetic field;
[III] Electrical detection of spin current;
[IV] Spin accumulation in a Rashba-type two-dimensional electron gas due to a nonuniform driving electric field;
[V] Persistent current and spin density in a mesoscopic Dresselhaus-type quantum ring;
[VI] Quantum scattering from a circular disk in a cubic-k Dresselhaus-type two dimensional electron gas;
[VII] Investigation on dissipationless edge state in the Quantum spin Hall system.

一、中文摘要:

在本計劃中，我們研究了操控半導體電子自旋的動力行為與傳輸的研究，其中包括(一)競爭性 Rashba 和 cubic-k Dresselhaus 本質自旋軌道交互作用對於產生自旋霍爾效應之影響探討；(二)內稟自旋霍爾效應在低磁場下的不對稱性；(三)自旋流之電性偵測；(四) 在 Rashba-type 二維電子氣中，由非均勻場所產生之自旋堆積；(五)介觀 Dreselhaus 量子環中的持續電流與自旋密度； (六)在動量立方相關的 Dresselhaus 二維電子氣中，圓形盤狀的量子散射；(七) 在量子自旋霍爾效應中的無耗散邊緣態研究。

(一)本論文主要興趣在於探討：於半導體系統中同時考量兩種本質自旋軌道交互作用（SOI）（Rashba SOI 與 Dresselhaus SOI）對於「自旋霍爾效應」產生的競爭性影響效果。其結果與作用機制可以直接反應在“邊界自旋堆積（S_z）”和“塊材自旋密度（S_i^B）”兩種可量性的物理量之表現。方法上，我們透過調制不同的自旋軌道交互作用耦合參數的相對強度比值，來加以系統性地研究自旋霍爾效應所對應到的不同依存性行為變化表現。其中最明顯的發現有（1.）於 Dresselhaus SOI 佔優勢的範疇中，S_z 會隨著電子密度的變化會而有明顯的變異，甚至於當電子密度夠大時，S_z 有改號現象發生。（2.）於 Rashba SOI 佔優勢的範疇中，S_z 則明顯受到抑制，其量值亦趨近於零（此與往前文獻研究中的預期結果完全符合）。

又如對於兩種各別本質自旋軌道交互作用優勢下所主導的特徵分佈範圍再進一步的分析，則可得知其 Rashba SOI 佔優勢的分際範圍在：(i) 對於 S_z，$\alpha \approx 2\tilde{\beta}$ (ii) 對於 S_i^B，$\alpha \geq \tilde{\beta}$。其中 $\alpha, \tilde{\beta}$ 為個別 Rashba SOI 與 線性-k Dresselhaus SOI 自旋軌道交互作用之耦合常數。此研究結果最重要意義的部分在於能揭示出：邊界自旋堆積(S_z)的明顯效應必須經由減弱 $|\alpha|$ 而予以回復與重現。

(二) 研究低磁場下二維條狀半導體的塊材自旋密度和邊緣自旋堆積行為；著重於 Dresselhaus 形式的內稟自旋軌道交互作用，我們發現在磁場平行或橫向於條狀傳輸方向會有對稱和不對稱的特性顯露出來。縱向的磁場會造成橫跨條狀樣品的自旋密度 S_z 產生奇宇稱，但對於磁場變化則是偶宇稱。橫向的磁場會造成橫跨條狀樣品的自旋密度 S_z 變成不對稱，對於磁場變化也是不對稱。我們結果可以用於鑑定不同自旋軌道交互作用的發生機制。

(三) 自旋電子學包含自旋注入、自旋傳輸、與量測。但是量測自旋流現今仍然是一個挑戰。在這裡將提出一種電性方法，去量測自旋流的大小。

(四)在外加一均勻電場下的擴散範疇中，Rashba 自旋軌道交互作用不會有自旋堆積產生(或自旋霍爾效應)。在這工作中，我們發現可以利用非均勻的場去回復自旋霍爾效應；我們考慮自旋霍爾效應在一個圓洞的邊緣，圓洞的半徑遠大於自旋弛豫長度，$R >> l_{so}$。而且自旋弛豫長度也遠大於電子自由路徑，$l_{so} >> l_e$。我們結果顯示非均勻場會產生平面的自旋密度 S_x ，S_y 導致他們可以藉由自旋擴散和進動產生一個有限的自旋電流，自旋堆積會正比於 Rashba 自旋軌道耦合係數 α，他的空間分布會垂直外加電場而呈現自旋偶極矩形式。

(五)最近，已經可以藉由分子束磊晶法長出 self-assembled 大範圍半徑差的半導體環。典型的樣品半截面顯示內徑約 10nm，而外徑介在 30nm 到 70 nm 之間。這種結構的位能應用已經被研究來當作自旋電子學和量子計算等。

(六) 解出二維 Dresselhaus 系統含 linear-k 與 cubic-k 的本徵值問題得到能量與波數射散關係。此外因為柱對稱的位能，本徵態必須以柱座標展開。考慮平面波入射無窮深位能二維盤 Dresselhaus 自旋軌道耦合系統。最後，可以討論 Rashba 與 linear-k Dresselhaus 的比較.

(七) 在量子霍爾效應中，邊緣態首次引起大家的興趣[1]。在強磁場下二維電子系統，電子行為沿著樣品邊緣出現迴旋軌道，而塊材行為像是絕緣體。邊緣的能階稱為藍道能階，由 $E_n = \hbar\omega_c\left(n+1/2\right)$ 來描述，$\omega_c = eB/m$ 為迴旋頻率。雖然此邊緣態有無耗散特性，但是在電子自旋元件中強磁場是應要被避免的。

2005 年，Kane and Mele 在石墨系統中提出不需加磁場的邊緣態，此也預測出新的效應---量子自旋霍爾效應。量子自旋霍爾系統中，在能帶間隙處於塊材裡而邊緣態為無間隙螺旋態。兩種相反自旋態沿著個邊緣以相反方向行進。由於自旋軌道交互作用在石墨裡太微弱，Benevig 等人在 HgTe/CdTe 半導體量子井中提出更實際的模型，並很快的被實驗所觀察且

證實。

Abstract:

We study the manipulation of electron spin dynamics and transport in the semiconductor:
[I] Competing interplay between Rashba and cubic-k Dresselhaus spin-orbit interactions in spin-Hall effect ; [II] Asymmetries in intrinsic spin-Hall effect in low in-plane magnetic field; [III] Electrical detection of spin current; [IV] Spin accumulation in a Rashba-type two-dimensional electron gas due to a nonuniform driving electric field; [V] Persistent current and spin density in a mesoscopic Dresselhaus-type quantum ring; [VI] Quantum scattering from a circular disk in a cubic-k Dresselhaus-type two dimensional electron gas; [VII] Investigation on dissipationless edge state in the Quantum spin Hall system.

[I] Competing interplay between Rashba and cubic-k Dresselhaus spin-orbit interactions in spin-Hall effect：

Focusing on the interplay between the Rashba and cubic-k Dresselhaus spin-orbit interactions (SOI), we calculate the spin accumulation S_z and the spin polarizations S_i^B at, respectively, the lateral edges and in the bulk of the two-dimensional electron gas. Their dependences on both the ratio between the Rashba and the Dresselhaus SOI coupling constants and the electron densities are studied systematically. Strong competition features in S_z are found. In the Dresselhaus-dominated regime S_z changes sign when the electron density is large enough. In the Rashba-dominated regime S_z is essentially suppressed. Most surprising is our finding that the Rashba-dominated regime occurs when $\alpha \approx 2\tilde{\beta}$, where α and $\tilde{\beta}$ are the Rashba and the effective linear-k Dresselhaus SOI coupling constants, respectively. For the spin polarizations S_i^B, the Rashba-dominated regime occurs when $\alpha \geq \tilde{\beta}$. Our results point out that decreasing $|\alpha|$ leads to the restoration of the spin accumulation S_z.

[II] Asymmetries in intrinsic spin-Hall effect in low in-plane magnetic field:

Effects of low in-plane magnetic field on bulk spin densities and edge spin accumulations of a diffusive two-dimensional semiconductor stripe are studied. Focusing upon the Dresselhaus-type intrinsic spin-orbit interaction (SOI), we look for the symmetry, or asymmetry, characteristics in two magnetic-field orientations: along and transverse to the stripe. For longitudinal field, the out-of-plane spin density S_z exhibits odd parity across the stripe and even parity in the magnetic field and is an edge accumulation. For transverse field, the out-of-plane S_z becomes asymmetric in both spatial and field dependencies and has finite bulk values for finite magnetic fields. Our results support utilizing low in-plane magnetic fields for the probing of the underlying SOI.

[III] Electrical detection of spin current:

Spintronics involve spin injection, transport and detection. Even though a lot of proposals on schemes for the measurement of spin current have been made, a feasible pure electrical means of measuring spin current remains a challenge. Here we theoretically demonstrate an electrical method to detect an ac spin current.

[IV] Spin accumulation in a Rashba-type two-dimensional electron gas due to a nonuniform driving electric field:

It is well understood that a Rashba-type two-dimensional electron gas (2DEG) does not support spin accumulation, or spin Hall effect, in the diffusive regime when the driving field is uniform. In this work we address the issue about a possible restoration of the spin Hall effect when the driving field becomes nonuniform. Toward this end, we consider the spin accumulation in the vicinity of a circular hole, with radius $R >> l_{so}$, where the driving field becomes nonuniform. Here l_{so} is the spin relaxation length, and $l_{so} \sim l_e$, the electron mean free path. Our results shows that the nonuniform driving field gives rise to nonuniform in-plane spin densities S_x and S_y which in turn contribute to a finite spin current via the combined processes of spin diffusion and spin-procession. The spin accumulation thus obtained is proportional to the Rashba coupling constant α, and its spatial pattern is one of spin-dipole form, aligned perpendicular to the driving field.

[V] Persistent current and spin density in a mesoscopic Dresselhaus-type quantum ring:

Recently, it is possible to grow self-assembled annulus semiconductor structures in a large range of inner and outer radii by using molecular beam epitaxy. Typical samples show a circular cross section with an inner radius about 10 nm, and the outer radius ranges between 30 and 70 nm. This kind of structures has been studied by their potential applications as spintronic and quantum computing. While most of the calculations have neglected the finite width of the ring, our interest is to look at the spin density distribution across the width and the net spin for a quantum state in the ring. Our finding is that the ring will carry a spontaneous magnetization when there is odd number of electrons in the ring, whereas in the case of a magnetic flux through the center of the ring, the ring will have spontaneous magnetization in most situations.

[VI] Quantum scattering from a circular disk in a cubic-k Dresselhaus-type two dimensional electron gas:

We will solve the eigenstate problem in two dimensional Dresselhaus-type system including linear-k and cubic-k. The eigenstates are represented by cylindrical functions due to the cylindrical symmetry potential. The cubic-*k* spin-orbit interaction causes the coupling between all the cylindrical functions. We attempt to introduce a semi-numerical method to solve for the eigenstates of the system, and to calculate the spin density in the vicinity of the circular potential disc.

[VII] Investigation on dissipationless edge state in the Quantum spin Hall system:

The first realization of propagating edge state is in the quantum Hall system.[1] In the presence of a strong magnetic field, the cyclotron-like orbital of electrons in a two-dimensional-electron-gas system will be deformed at the sample edges into propagating edge states of energy higher than the Landau level in the bulk. At this energy, there is no bulk state and so the bulk behaves as an insulator. These edge states have a nice dissipationless property. However, the need of a strong magnetic field for the setting up of the state is not a welcoming feature for application purpose. In 2005, Kane and Mele[2] proposed another edge state, which does not require a magnetic field, in the graphene system. This new phenomenon is now known as the quantum spin Hall (QSH)

effect. QSH system has an energy gap in the bulk, but has gapless helical edge states with opposite spins counter-propagating at each edge. More recently, Benevig et al.[3] propose a more realistic material for the edge state physics: the semiconductor HgTe/CdTe quantum wells. An experimental confirmation of part of the prediction of QSH is soon demonstrated in a ballistic edge channels[4] We study the edge state physics as will be revealed by s local scatterer.

[1] K. V. Klitzing et al., Phys. Rev. Lett. 45, 494 (1980).
[2] C. L. Kane and E. J. Mele, Phys. Rev. Lett. 95, 226801 (2005).

Keywords:
Nonuniform field, low magnetic field, diffusion, spin Hall effect, spin accumulation, cubic Dresselhaus, Rashba, spin-orbit interaction, spin current, electrical detection, persistent current, quantum ring, cylindrical symmetry, hard-wall disk, quantum spin-Hall effect, dispersionless, edge state.

二、Motivations and goals

[I] Competing interplay between Rashba and cubic-k Dresselhaus spin-orbit interactions in spin-Hall effect：

Spin-orbit interaction (SOI) provides the key leverage for the recent strive for all electrical generations and manipulations of spin densities in semiconductors. [1-9] Intrinsic SOIs, such as the Rashba SOI (RSOI) [1, 7, and 9–10] and the Dresselhaus SOIs (DSOIs) [6], are of particular interest. It is due to their tunability, gate tuning for the RSOI and either sample thickness or electron-density tuning for the DSOI, and to their physical origins, being independent of disorder that requires the presence of SOI impurities. Yet the ever present background scatterers do play a subtle role in the intrinsic spin-Hall effect [11]. In spin-Hall effect (SHE), an external electric field induces a transverse spin current and, in turn, an out-of-plane spin accumulation S_z at lateral edges [1,5–9]. For intrinsic SOIs, the background scatterers lead to a complete quenching of the edge spin accumulation S_z when the SOI depends only linearly on the electron momentum k [11], but S_z maintains finite and dependent on the momentum relaxation time τ when the SOI has a cubic-k dependence [11–14]. Thus, separately considered, the RSOI does not contribute to edge spin accumulation S_z while the cubic-k DSOI does. For a more realistic situation, when the two SOIs coexist in a sample, RSOI could exert its effect on the edge spin accumulation S_z, but that would have to be mediated through the cubic-k DSOI. It is of great interest to see whether this effect would be reinforcing or competing for S_z.

Thus, in this work, we focus upon the interplay between the RSOI and the cubic-k DSOIs in their combined, or competing, effects on both the edge spin accumulation S_z and the bulk spin density S_i^B. Bulk spin density S_i^B, formed in an external electric field, is another important physical quantity of interest that is closely related to the intrinsic SOIs. The subscript i denotes the vector component of spin. The effect of the background scatterers on S_i^B is less subtle than that on S_z : S_i^B, remains finite for all intrinsic SOIs and depends on τ also.[3] Intuitively, up to leading order in the SOI coupling constant one might expect this S_i^B feature to arise from a SOI-effective magnetic field.[4] It turns out to be the case when there is only one dominated SOI and the SOI depends on k linearly. Take, for instance, a Rashba-type two dimensional electron gas _2DEG_ in the diffusive regime, the k-dependent effective magnetic field becomes $<\boldsymbol{h}_k>=-\alpha\hat{\boldsymbol{z}}\times\boldsymbol{E}$ when $<\boldsymbol{k}>$ is averaged over the electron distribution given by a shifted Fermi sphere $f(\varepsilon,\boldsymbol{k})=f_0(\varepsilon,\boldsymbol{k})-\frac{\tau e\hbar\,\boldsymbol{k}\bullet\boldsymbol{E}}{m^*}\delta(\varepsilon_F-\varepsilon)$ where α, f_0, and m^* are, respectively, the Rashba coupling constant, Fermi-Dirac distribution, and electron mass and for e0. With $<\boldsymbol{h}_k>=\alpha\tau e/\hbar\hat{\boldsymbol{z}}\times\boldsymbol{E}$, the bulk spin density, in units of , is given by $\boldsymbol{S}^B=-N_0\alpha\tau e/\hbar\hat{\boldsymbol{z}}\times\boldsymbol{E}$, which was first obtained by Edelstein.3 In the above expression the density of states per spin is denoted by N_0. Beyond leading order or linear k dependence in the SOIs, or for the coexistence of different types of SOIs, the derivation of S_i^B becomes more involved. In this work, we calculate the S_i^B within a spin-diffusion equation approach and perform a systematic study on the competing interplay between the RSOI and the cubic-k SOIs. This work is accepted for publication in Physical Review B within two months.

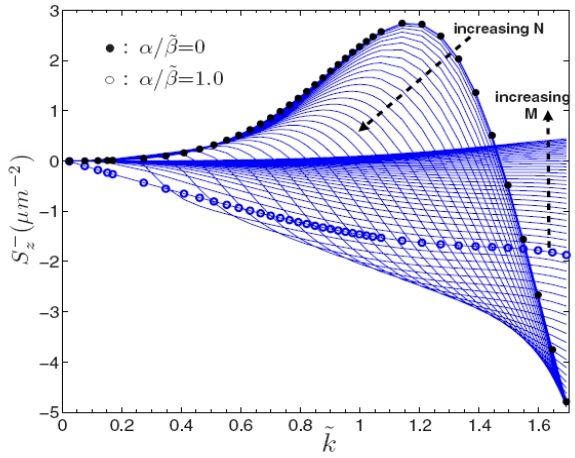

FIG. 3. (Color online) Spin densities S_z^- versus $\tilde{k}$. The case of pure Dresselhaus SOI ($\alpha/\tilde{\beta}$=0) is denoted by black circular dots. The case of $\alpha/\tilde{\beta}$=1.0 is indicated by blue open circles. Intermediate between them we have curves for $\alpha/\tilde{\beta}=N\times\Delta$, where $\Delta=\frac{1}{32}$. From $\alpha/\tilde{\beta}$=1 to $\alpha/\tilde{\beta}$=2 we have curves for $\alpha/\tilde{\beta}=1+M\times\Delta$. S_z^- is essentially suppressed when $\alpha\approx 2\tilde{\beta}$.

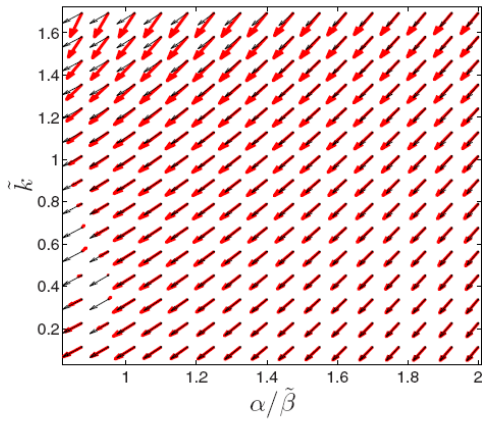

FIG. 5. (Color online) Bulk spin polarization S^B as a function of $\alpha/\tilde{\beta}$ and $\tilde{k}$, and for $0.9\leq\alpha/\tilde{\beta}\leq 2.0$.

[1] M. I. Dyakonov and V. I. Perel, Phys. Lett. 35A, 459 (1971).
N. S. Averkiev and M. I. Dyakonov, JETP Lett., 196(1983).

[2]A. A. Bakun, B. P. Zakharchenya, A. A. Rogachev, M. N. Tkachuk, V. G. Fleisher, JETP Lett. 40, 1293 (1984).

[3]V. M. Edelstein, Solid State Commun. 73, 233 (1990).

[4]A. G. Aronov, Yu. B. Lyanda-Geller, and G. E. Pikus, Sov. Phys. JETP 73, 537 (1991).

[5]J. E. Hirsch, Phys. Rev. Lett. 83, 1834 (1999).

[6]S. Murakami, N. Nagaosa, and S. C. Zhang, Science 301, 1348 (2003).

[7]J. Sinova, D. Culcer, Q. Niu, N. A. Sinitsyn, T. Jungwirth, and A. H. MacDonald, Phys. Rev. Lett. 92, 126603 (2004).

[8]Y. K. Kato, R. C. Myers, A. C. Gossard, and D. D. Awschalom, Science 306, 1910 (2004).

[9]J. Wunderlich, B. Kaestner, J. Sinova, and T. Jungwirth, Phys. Rev. Lett. 94, 047204 (2005).

[10]E. I. Rashba, Sov. Phys. Solid State 2, 1109 (1960); Yu. A. Bychkov and E. I. Rashba, JETP Lett. 39, 78 (1984).

[11] J. I. Inoue, G. E. W. Bauer, and L. W. Molenkamp, Phys. Rev. B 70, 041303(R) (2004); E. G. Mishchenko, A. V. Shytov, and B. I. Halperin, Phys. Rev. Lett. 93, 226602 (2004); A. A. Burkov, A. S. Núñez, and A. H. MacDonald, Phys. Rev. B 70, 155308 (2004); R. Raimondi and P. Schwab, Phys. Rev. B 71, 033311, (2005); O. V. Dimitrova, Phys. Rev. B 71, 245327 (2005).

[12]A. G. Malshukov and K. A. Chao, Phys. Rev. B 71, 121308(R) (2005).

[13]B. A. Bernevig and S. C. Zhang, Phys. Rev. Lett. 95, 016801 (2005).

[14]A. G. Mal'shukov, L. Y. Wang, C. S. Chu, and K. A. Chao, Phys. Rev. Lett. 95, 146601 (2005).

[II] Asymmetries in intrinsic spin-Hall effect in low in-plane magnetic field:

Out-of-plane spin polarization is of particular interest because it permits efficient optical probe by Kerr rotation. The edge spin accumulation, according to the spin-Hall effect (SHE), has an out-of-plane component and is resulted from a transverse spin current induced by the electric field.[1-4] However, for the case of intrinsic SOI, it is understood that the SHE is quenched by background scatterers, be they isotropic or anisotropic, [5] as long as the intrinsic SOIs consist of only linear-momentum dependence term. Meanwhile, no out-of-plane bulk spin densities are expected in an electric field.[6] When applying an in-plane magnetic field to a two-dimensional (2D) system, one might be led by the inplane nature of the effective spin-orbit magnetic field $\vec{h}_{eff} = <\vec{h}_k> \neq 0$, obtained by averaging the spin-orbit effective field over the distribution of the electron momentum $\hbar\vec{k}$, to expect that there were no out-of-plane spin densities. This is shown not to be the case by Engel *et al.* [7] for a Rashba-type 2D system, where out-of-plane spin densities are found when the external in-plane magnetic field is longitudinal: a configuration studied by recent experiments. [8,9] However, either the scatterer has to be anisotropic or the electron dispersion has to be nonparabolic for the effect to hold. [7] Here, longitudinal denotes the direction parallel to the electric field and its orthogonal counterpart in the 2D plane is denoted transverse.

In this paper, we have shown that out-of-plane bulk spin density can be generated in another system configuration with less restrictive assumptions. The configuration is a Dresselhaus-type 2D system and the external in-plane magnetic field is in a transverse orientation. More importantly, the effect holds for isotropic background scatterers and for parabolic dispersion for electrons. Our calculation has included the cubic Dresselhaus SOI. This work is published in Physical Review B.

[1] M. I. Dyakonov and V. I. Perel, Phys. Lett. **35A**, 459 _1971_.

[2] S. Murakami, N. Nagaosa, and S. C. Zhang, Science **301**, 1348 (2003).

[3] J. Sinova, D. Culcer, Q. Niu, N. A. Sinitsyn, T. Jungwirth, and A. H. MacDonald, Phys. Rev. Lett. **92**, 126603 (2004).

[4] Y. K. Kato, R. C. Myers, A. C. Gossard, and D. D. Awschalom, Science **306**, 1910 (2004).

[5] J. I. Inoue, G. E. W. Bauer, and L. W. Molenkamp, Phys. Rev. B **70**, 041303R (2004); E. G. Mishchenko, A. V. Shytov, and B. I. Halperin, Phys. Rev. Lett. **93**, 226602 (2004).

[6] V. M. Edelstein, Solid State Commun. **73**, 233 (1990).

[7] H. A. Engel, E. I. Rashba, and B. I. Halperin, Phys. Rev. Lett. **98**, 036602 (2007).

[8] Y. K. Kato, R. C. Myers, A. C. Gossard, and D. D. Awschalom, Phys. Rev. Lett. **93**, 176601 (2004).

[9] N. P. Stern, S. Ghosh, G. Xiang, M. Zhu, N. Samarth, and D. D. Awschalom, Phys. Rev. Lett. **97**, 126603 (2006).

[III] Electrical detection of spin current:

Spintronics involve spin injection, transport and detection. Even though many people propose many means to measure spin current, but how to detect spin current is still a challenge now. Here we theoretically demonstrate an electrical method to detection the magnitude of in-plane spin current.

We proposal a device with 2DEG (two dimensional electron gas) sandwiched in between two parallel metallic plate as is given in the following picture.

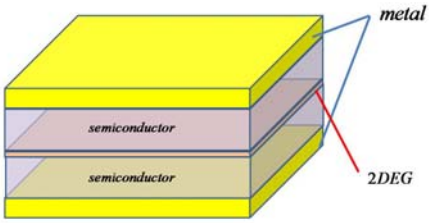

Our calculation starts from the perturbed spin-orbit interaction term of the Hamiltonian.

$$H' = e\frac{\Lambda}{\hbar}\vec{\sigma}\bullet\left(\vec{p}\times\vec{E}\right)$$

where e is the magnitude of electron charge; Λ is the spin-orbit interaction constant; $\hbar$ is the plank constant; $\vec{\sigma}$ is the Pauli matrices ; E is the electric field.

By averaging the perturbed Hamiltonian H' by the spin polarized electron wave function, we obtain the effective perturbed Hamiltonian H'_{eff} for the photons. When the electron is allowed to flow, the effective perturbed Hamiltonian will describe the emission of photon by the AC spin current. Using the perturbed Hamiltonian H'_{eff}, we can obtain the one photon emission wave function of the photons. This allows us to calculate the expectation value of the vector potential ,

$$\vec{A}\left(\vec{r},t\right) = \left\langle \Psi \left| A^{(op)} \right| \Psi \right\rangle$$

From which we can calculate the electric field. For our setting, the electric field we are looking at is in between two infinite conducting plates sandwiching the 2DEG on which the spin current is located. By integrating the electric field, we obtain the electric potential difference between the two metallic plants. For a reasonable choice of system parameters, the voltage across the metal plates is of the order of 10 nA, which is within the comfortable range of the present experimental capability. This work is intended to submit to Physical Review Letters.

[IV] Spin accumulation in a Rashba-type two-dimensional electron gas due to a nonuniform driving electric field:

The SHE induces transverse spin currents towards opposite directions with opposite spins via a longitudinal driving field with SOI. The extrinsic SHE arises from the skew scattering process due to the spin-dependent impurity.[1] The opposite out-of-plane spin accumulations at lateral edges can be probed by Kerr rotation due to the extrinsic SHE.6 In contrast, the intrinsic SHE is contributed from SOI band dependence such as the Rashba SOI (RSOI) or the Dresselhaus SOI

(DSOI). These SOIs are related to electron momentum k from the $\mathbf{k}\cdot\mathbf{p}$ band calculation. Furthermore, the generation of the intrinsic SHE in the diffusive regime becomes a key issue and the SHE can be induced against impurities through the cubic DSOI.[2] However, in the presence of disorder, including either isotropic or anisotropic impurities,[3] the intrinsic SHE is quenched for the linear RSOI. In highly symmetric system, the finite spin current can form a finite spin accumulation near the boundary.[4,5] In the diffusive regime with RSOI, the SHE can be restored by considering the anisotropic scatterers, or non-parabolic electron dispersion with an in-plane magnetic field, or by the magnetic means. The nonuniform driving field achieved by asymmetric mesoscopic structures can generate the spatial variation of the spin polarization near the boundary. In this paper, we start from the diffusion approximation based on electron transport to derive the drift-diffusion equations where spin and charge densities are coupled to each other via the SOI. The boundary conditions are connected to spin currents by spin and charge densities and it causes the spin accumulation. This work is to be submitted for publication.

[1] H. A. Engel, B. I. Halperin, and E. I. Rashba, Phys. Rev. Lett. **95**, 166605 (2005).

[2] A. G. Mal'shukov and K. A. Chao, Phys. Rev. B 71, 121308(R) (2005).

[3] J. I. Inoue, G. E. W. Bauer, and L. W. Molenkamp, Phys. Rev. B 70, 041303(R) (2004); A. A. Burkov, A. S. Nunez, and A. H. MacDonald, Phys. Rev. B 70, 155308 (2004); R. Raimondi and P. Schwab, Phys. Rev. B 71, 033311 (2005); O. V. Dimitrova, *ibid* . 71, 245327 (2005); B. A. Bernevig and S. C. Zhang, Phys. Rev. Lett. 95, 016801 (2005).

[4] A. G Mal'shukov, L. Y. Wang, C. S. Chu, and K. A. Chao, Phys. Rev. Lett. 95, 146601 (2005).

[5] Dimitrie Culcer and R. Winkler, Phys. Rev. Lett. 99, 226601 (2007).

[V] Persistent current and spin density in a mesoscopic Dresselhaus-type quantum ring:

The geometric model of our research is an isolated finite width mesoscopic ring with Dresselhaus spin-orbit (DSO) coupling. The cross section of the structure is shown in Fig.1.

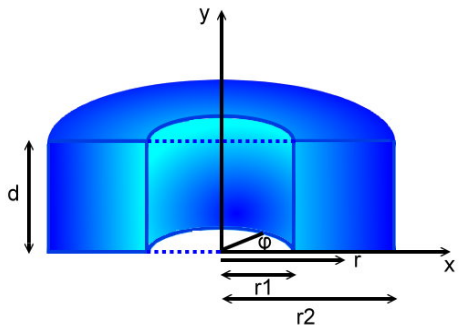

Fig.1 The figure is the cross section of the finite width mesoscopic ring, where r_1 and r_2 are the inner and outer radii.

If we just consider the k-linear bulk inversion asymmetry (BIA) contribution, the total single-particle Hamiltonian for a quantum ring (QR) which we assume a narrow QR with the z direction grown along [001] and present the total Hamiltonian in matrix form, we

get $H \simeq \begin{pmatrix} \frac{\hat{p}^2}{2m^*}+V & i\beta(\frac{\pi}{d})^2 e^{i\phi} p^+_{\rho,\phi} \\ i\beta(\frac{\pi}{d})^2 e^{-i\phi} p^-_{\rho,\phi} & \frac{\hat{p}^2}{2m^*}+V \end{pmatrix}$

, where $k_\pm = -ie^{\pm i\phi}\left[\frac{\partial}{\partial\rho} \pm i\frac{1}{\rho}\frac{\partial}{\partial\phi}\right] \equiv -ie^{\pm i\phi} p^\pm_{\rho,\phi}$; m^* is the electron effective mass; $V(\vec{r},z)$ is the spatial confinement for $\vec{r}=(x,y)$ and z along the ring axis; β is the Dresselhaus SO constant for the material.

After demonstration and numerical analysis, we can discuss the energy-splitting induced by the magnetic flux, spin accumulation and persistent current. Furthermore, we can design the quantum computing devices in the future work.

[VI] Quantum scattering from a circular disk in a cubic-k Dresselhaus-type two dimensional electron gas:

The most important is the method of partial waves. The total wave is composed of incoming waves and outgoing waves where the incoming wave part is given by the incident plane wave and then outgoing wave part can be represented by the eigenstate which we obtain before. Furthermore, the outgoing wave part contains unknown coefficients which are resulted from the two kinds of helicity wave functions. The unknown coefficients can be obtained by solving the boundary condition problems. Finally, we obtain the particle current density by driving the particle continuity equation of the Dresselhaus-type system.

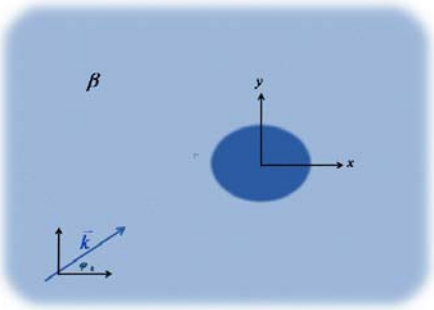

Figure 2.3: The plane wave of an incident electron wave with wave vector k maling an angle ϕ_k with $\hat{X}$ axis gets scattered by a scattering region defined by a Dresselhaus SOI and a "hard" wall disk .

If we just consider the k-linear bulk inversion asymmetry (BIA) contribution, the total single-particle Hamiltonian for a quantum ring (QR) which we assume a narrow QR with the z direction grown along [001] and present the total Hamiltonian in matrix form, we

get $H \simeq \begin{pmatrix} \frac{\hat{p}^2}{2m^*}+V & i\beta(\frac{\pi}{d})^2 e^{i\phi} p^+_{\rho,\phi} \\ i\beta(\frac{\pi}{d})^2 e^{-i\phi} p^-_{\rho,\phi} & \frac{\hat{p}^2}{2m^*}+V \end{pmatrix}$

, where $k_\pm = -ie^{\pm i\phi}\left[\frac{\partial}{\partial\rho} \pm i\frac{1}{\rho}\frac{\partial}{\partial\phi}\right] \equiv -ie^{\pm i\phi} p^\pm_{\rho,\phi}$; m^* is the electron effective mass; $V(\vec{r},z)$ is the spatial confinement for $\vec{r}=(x,y)$ and z along the ring axis; β is the Dresselhaus SO constant for

the material.
After demonstration and numerical analysis, we can discuss the energy-splitting induced by the magnetic flux, spin accumulation and persistent current. Furthermore, we can design the quantum computing devices in the future work.

[VII] Investigation on dissipationless edge state in the Quantum spin Hall system:
However, there are still several problems need to be solved, e.g. how robust the edge state is against the disorder? Does reflection happen when the edge state comes to one corner but two different spin orientations along two direction edges? How to utilize the spin-resolved edge when the absence of magnetic field preserving the time reversal symmetry leads to a Kramer degeneracy and zero net charge and spin current...etc. ?

We investigate these problems with effective four-band model derived from the Kane model for semiconductors confining in a heterojunction of semiconductor HgTe/CdTe.[1] The Hamiltonian is descried by $H = \begin{pmatrix} h(k) & 0 \\ 0 & h^*(-k) \end{pmatrix}$ where

$h(k) = \varepsilon(k) I_{2\times 2} + d_i \sigma^i$, $\varepsilon(k) = C - D\left(k_x^2 + k_y^2\right) = \varepsilon(k) = C - Dk^2$,

$d_i(k) = \left(Ak_x, Ak_y, M(k)\right)$ and $M(k) = M - B\left(k_x^2 + k_y^2\right) = M - Bk^2$. $h*$ is time reversal of h. A, B, C, D, and M are the parameters determined by the thickness of the quantum well. The crucial parameter is mass or gap parameter M changes its sign when the thickness d of the quantum well is varied through a critical thickness d_c =6.3 (nm). The quantum well has QSH phase in case of $d>d_c$ and normal insulator phase in case of $d<d_c$. [3]

[1] B. A. Bernevig et al., Science 314, 1757 (2006).
[2] M. König et al., Science 318, 766 (2007);
[3] Pfeuffer-Jeschke, Ph.D. thesis thesis, University of Würzburg (2000).

三、Results and discussion:

[I] Competing interplay between Rashba and cubic-k Dresselhaus spin-orbit interactions in spin-Hall effect (Appendix A).

[II] Asymmetries in intrinsic spin-Hall effect in low in-plane magnetic field (Appendix B).

[IV] Spin accumulation in a Rashba-type two-dimensional electron gas due to a nonuniform driving electric field

For RSOI case, the uniform driving electric field can induce the uniform in-plane spin density but the nonuniform driving electric field can induce the nonuniform in-plane particular spin density S_i^p. S_i^p can contribute a finite spin current such that the out-of-plane spin accumulation is built-up to compensate this spin current near the boundary. In general, the spin drift-diffusion equations for the intrinsic SHE can be expressed by [4]

$$\sum_{j=x,y,z}\left[\delta^{ij}D\nabla^2+R^{ijm}\nabla_m-\Gamma^{ij}\right]S_j+M^{i0}D_0^0/2=0. \qquad (1)$$

The diffusion constant is $D=v_F^2\tau/2$ with the Fermi velocity v_F and elastic scattering time τ.

The spin dynamics can consider by the first conventional diffusion term, the spin precession term related to R^{ijm}, D'yakonov-Perel' (DP) spin relaxation term related to Γ^{ij}, and the source term M^{i0} contributed from the spin-charge coupling due to SOI. The electric potential φ(r) enters into Eq. (1) only through $D_0{}^0=2eN_0\varphi$, where the electric field is E(r)= -▽φ(r). Furthermore, the spin-charge source term can be removed by introducing $\Delta S_j=S_j-S_j^p$ replacing S_j in Eq. (1). For intrinsic SHE, the in-plane nonuniform electric field E(r) can induce the position-dependent $S^p{}_{x(y)}$ via the spin-charge source term. On the other hand, the in-plane E(r) does not induce the out-of-plane spin polarization resulting in $S^p{}_z=0$.

We denoting I_n^j is the spin current projected on $\hat{n}$-direction, where $\hat{n}=(\cos\phi,\sin\phi)$ is the unit vector normal to the boundary and ϕ is the angle between $\hat{n}$ and x axis. I_n^j is connected to the total spin density S_i in the expression of

$$I_n^{i=x,y}=-2D\nabla_n S_i-R^{izi}S_z\hat{n}\bullet\hat{i} \qquad (2)$$

where $\nabla_n=\cos\phi(\partial/\partial x)+\sin\phi(\partial/\partial y)$. When the hard-wall boundary is imposed in our system, it implies that spin currents are equal to zero in Eq. (2). Apparently, the spin density $S_j=\Delta S_j+S_j^p$ is position-dependent because the nonuniform electric field induces the nonuniform S_j^p. Consequently, $\nabla_n S_i\neq 0$ allows a finite spin accumulation S_z to compensate its contribution in Eq. (2) at the boundary.

To study the phenomenon of the nonuniform driving field applied to the spin diffusion equation acted upon the RSOI, we adopt a realistic model of a circular hole with radius R_0. While a driving electric field $E_0\hat{x}$ is applied, *Sz* presents the dipole spatial distribution in Fig. 1. The maximum spin-up (-down) polarization occurs at $\phi=3\pi/2(\pi/2)$ and it decreases within a

range of 1.1 μm.

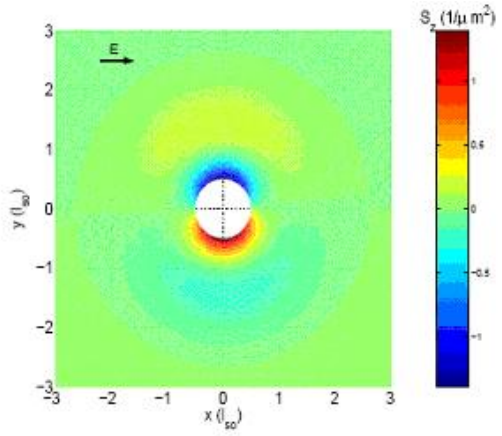

Fig1: Spatial distribution of spin density S_z around a hole with a radius 1.8 μm.

Appendix A:

PHYSICAL REVIEW B **79**, 195314 (2009)

Competing interplay between Rashba and cubic-*k* Dresselhaus spin-orbit interactions in spin-Hall effect

R. S. Chang,[1] C. S. Chu,[1,2] and A. G. Mal'shukov[1,2,3]
[1]*Department of Electrophysics, National Chiao Tung University, Hsinchu 30010, Taiwan*
[2]*National Center for Theoretical Sciences, Physics Division, Hsinchu 30043, Taiwan*
[3]*Institute of Spectroscopy, Russian Academy of Science, 142190 Troitsk, Moscow oblast, Russia*
(Received 5 March 2009; revised manuscript received 20 April 2009; published 14 May 2009)

Focusing on the interplay between the Rashba and cubic-*k* Dresselhaus spin-orbit interactions (SOI), we calculate the spin accumulation S_z and the spin polarizations S_i^B at, respectively, the lateral edges and in the bulk of the two-dimensional electron gas. Their dependences on both the ratio between the Rashba and the Dresselhaus SOI coupling constants and the electron densities are studied systematically. Strong competition features in S_z are found. In the Dresselhaus-dominated regime S_z changes sign when the electron density is large enough. In the Rashba-dominated regime S_z is essentially suppressed. Most surprising is our finding that the Rashba-dominated regime occurs when $\alpha \approx 2\tilde{\beta}$, where α and $\tilde{\beta}$ are the Rashba and the effective linear-*k* Dresselhaus SOI coupling constants, respectively. For the spin polarizations S_i^B, the Rashba-dominated regime occurs when $\alpha \geq \tilde{\beta}$. Our results point out that decreasing $|\alpha|$ leads to the restoration of the spin accumulation S_z.

DOI: 10.1103/PhysRevB.79.195314 PACS number(s): 72.25.Dc, 71.70.Ej, 75.40.Gb, 85.75.−d

I. INTRODUCTION

Spin-orbit interaction (SOI) provides the key leverage for the recent strive for all electrical generations and manipulations of spin densities in semiconductors.[1–9] Intrinsic SOIs, such as the Rashba SOI (RSOI) (Refs. 3, 7, and 9–12) and the Dresselhaus SOIs (DSOIs),[6,13,14,23] are of particular interest. It is due to their tunability, gate tuning for the RSOI and either sample thickness or electron-density tuning for the DSOI, and to their physical origins, being independent of disorder that requires the presence of SOI impurities. Yet the ever present background scatterers do play a subtle role in the intrinsic spin-Hall effect.[15] In spin-Hall effect (SHE), an external electric field induces a transverse spin current and, in turn, an out-of-plane spin accumulation S_z at lateral edges.[1,5–9] For intrinsic SOIs, the background scatterers lead to a complete quenching of the edge spin accumulation S_z when the SOI depends only linearly on the electron momentum k,[15] but S_z maintains finite and dependent on the momentum relaxation time τ when the SOI has a cubic-*k* dependence.[14–17] Thus, separately considered, the RSOI does not contribute to edge spin accumulation S_z while the cubic-*k* DSOI does. For a more realistic situation, when the two SOIs coexist in a sample, RSOI could exert its effect on the edge spin accumulation S_z, but that would have to be mediated through the cubic-*k* DSOI. It is of great interest to see whether this effect would be reinforcing or competing for S_z.

Thus, in this work, we focus upon the interplay between the RSOI and the cubic-*k* DSOIs in their combined, or competing, effects on both the edge spin accumulation S_z and the bulk spin density S_i^B. Bulk spin density S_i^B, formed in an external electric field, is another important physical quantity of interest that is closely related to the intrinsic SOIs. The subscript i denotes the vector component of spin. The effect of the background scatterers on S_i^B is less subtle than that on S_z: S_i^B, remains finite for all intrinsic SOIs and depends on τ also.[3] Intuitively, up to leading order in the SOI coupling constant one might expect this S_i^B feature to arise from a SOI-effective magnetic field.[4] It turns out to be the case when there is only one dominated SOI and the SOI depends on k linearly. Take, for instance, a Rashba-type two-dimensional electron gas (2DEG) in the diffusive regime, the k-dependent effective magnetic field becomes $\langle \mathbf{h_k} \rangle = -\alpha \mathbf{z} \times \langle \mathbf{k} \rangle$ when $\langle \mathbf{k} \rangle$ is averaged over the electron distribution given by a shifted Fermi sphere $f(\epsilon, \mathbf{k}) = f_0(\epsilon, \mathbf{k}) - \frac{\tau e \hbar \mathbf{k} \cdot \mathbf{E}}{m^*} \delta(\epsilon_F - \epsilon)$, where α, f_0, and m^* are, respectively, the Rashba coupling constant, Fermi-Dirac distribution, and electron mass and for $e > 0$. With $\langle \mathbf{h_k} \rangle = \alpha \tau e / \hbar \hat{\mathbf{z}} \times \mathbf{E}$, the bulk spin density, in units of $\hbar$, is given by $\mathbf{S}^B = -N_0 \alpha \tau e / \hbar \hat{\mathbf{z}} \times \mathbf{E}$, which was first obtained by Edelstein.[3] In the above expression the density of states per spin is denoted by N_0. Beyond leading order or linear k dependence in the SOIs, or for the coexistence of different types of SOIs, the derivation of S_i^B becomes more involved. In this work, we calculate the S_i^B within a spin-diffusion equation approach and perform a systematic study on the competing interplay between the RSOI and the cubic-*k* SOIs.

Interplay between the RSOI and the linear-*k* DSOI in a sample has attracted much attention lately.[18–29] Earlier work studied the effect of $\alpha = \tilde{\beta}$, where $\tilde{\beta}$ is the effective linear-*k* DSOI coupling constant, on the magnetoconductivity.[18] More recent work on the same $\alpha = \tilde{\beta}$ regime pointed out that the spin becomes a good quantum number, independent of k, and has a long relaxation time.[19] The D'yakonov-Perel' (DP) mechanism[1] for spin relaxation is suppressed. This finding led to proposals for spintronic transistor that would manipulate polarized spin transport in the diffusive regime.[19,20] It was later shown, within the same $\alpha/\tilde{\beta} = 1$ regime, that the Fermi circles of opposite spins are connected by a wave vector $\mathbf{Q}$ that depends only on the SOI constant and the effective mass.[24] This leads to the persistent spin-helix state.[24] Since the ratio $\alpha/\tilde{\beta}$ is important for the development of spintronics, and the transport is anisotropic when both α and $\tilde{\beta}$ are

finite,[22,23,26–29] a number of experiments were designed to extract this ratio by the monitoring of the spin photocurrent.[22,26,27] Most of the studies dealt with the linear-k SOIs. One of the exceptions is a weak localization experiment that has extracted α, $\tilde{\beta}$, and also the cubic-k DSOI coupling constant from comparing the magnetoconductance data with a weak localization theory.[21] The delicate interplay between the RSOI and the cubic-k DSOI is yet to be explored and is much needed in either the spin transport, as is briefed above, or in the spin accumulations, as is related to SHE.

To study the interplay between the RSOI and the cubic-k DSOI in the diffusive regime, we extend our previous studies on the spin diffusive in a 2DEG strip to include both types of the SOI.[17] The diffusive regime has $l_e < L_{\rm so}$, where $L_{\rm so}$ and l_e are, respectively, the typical spin-relaxation length due to either the RSOI or the DSOI and the momentum-relaxation length. We study in detail the variations in S_z and S_i^B with respect to $\alpha/\tilde{\beta}$ and to the electron density. Our result shows Dresselhaus-dominated and Rashba-dominated regimes are determined primarily by the ratio $\alpha/\tilde{\beta}$. In the intermediate regime, intricate interplay between the RSOI and cubic-k DSOI is clearly shown as the electron density is varied. The edge spin accumulation S_z is essentially suppressed in the Rashba-dominated regime. Most surprisingly is our finding that the Rashba-dominated regime occurs when $\alpha \approx 2\tilde{\beta}$ for the edge spin accumulation S_z and when $\alpha = \tilde{\beta}$ for the bulk spin polarization S_i^B. Our result points to a possible way to restore the DSOI's contribution to the SHE, namely, to lower $|\alpha/\tilde{\beta}|$ to values well below unity. In Sec. II we present the spin-diffusion equation and the analytical solutions. In Sec. III we present our numerical results and discussions. Finally, in Sec. IV, we will present our conclusion.

II. THEORY

The system we consider is a 2DEG confined in an infinite strip with transverse boundaries at $y = \pm d/2$. The thickness of the strip $w \ll d$. An electric field $\mathbf{E}$ in the x direction induces the SHE. The phenomenon is described by a spin-diffusion equation[14,17] which has been derived from the Keldysch nonequilibrium Green's function method.[30] It has also been extended to the case of an in-plane magnetic field.[31] Detail of the derivation is not repeated here, but we will describe the physical meaning of the terms in the spin-diffusion equation. For our purpose here, the SOI magnetic field $\mathbf{h_k}$ includes both the RSOI and the cubic-k DSOI and is separated into linear-k and cubic-k terms $\mathbf{h_k} = \mathbf{h_{k,1}} + \mathbf{h_{k,3}}$. In a 2DEG, $\mathbf{h_k}$ lies on the two-dimensional plane after we average it with the lowest subband wave function over its thickness. Explicitly, we have

$$\mathbf{h}_{\mathbf{k},1} = \alpha(k_y, -k_x) + \beta\kappa^2(-k_x, k_y),$$

$$\mathbf{h}_{\mathbf{k},3} = \beta(k_x k_y^2, -k_y k_x^2). \tag{1}$$

Here, β is the DSOI coupling constant, $\kappa^2 = \langle k_z^2 \rangle$, and k_x and k_y are along, respectively, the [100] and [010] directions for a zinc-blende crystal.[32] It is convenient to define the effective linear-k DSOI coupling constant $\tilde{\beta} = \beta\kappa^2$. The SOI hamiltonian $\mathbf{H}_{\rm so} = \mathbf{h_k} \cdot \boldsymbol{\sigma}$, where $\boldsymbol{\sigma}$ is the Pauli-matrix vector.

Equation (1) provides us a simple way to get at the direction of the effective magnetic field $\mathbf{h_k}$ for a given electron distribution in the $\mathbf{k}$ space. This is important for an intuitive understanding of the spin-diffusion equation. From $\mathbf{h_k} = -\mathbf{h_{-k}}$, the effective magnetic field is zero when the $\mathbf{k}$-space occupation is symmetric, as it is for the equilibrium case. If the deviation from equilibrium is a shifted distribution characterized by a wave vector $\mathbf{Q}$, then the effective magnetic field $\mathbf{h}^R$ due to RSOI will be along the direction of $\hat{\mathbf{Q}} \times \hat{\mathbf{z}}$. The DSOI case is less straight forward, but when $\mathbf{Q}$ is along either k_x or k_y, then $\mathbf{h}^D$ will be along or opposite to $\hat{\mathbf{Q}}$. Specifically, in the low electron-density ($k_F \ll \kappa$) regime $\mathbf{h}^D$ will be opposite (along) to $\mathbf{Q}$ when $\mathbf{Q}$ is along k_x (k_y). The direction of $\mathbf{h}^D$ will be reversed in the high-density ($k_F \gg \kappa$) regime. Here k_F is the Fermi wave vector.

The stationary spin-diffusion equations are given by

$$D\frac{\partial^2}{\partial y^2}S_z + \frac{R^{zxy}}{\hbar}\frac{\partial}{\partial y}S_x + \frac{R^{zyy}}{\hbar}\frac{\partial}{\partial y}S_y - \frac{\Gamma^{zz}}{\hbar^2}S_z = 0,$$

$$D\frac{\partial^2}{\partial y^2}S_y + \frac{R^{yzy}}{\hbar}\frac{\partial}{\partial y}S_z - \frac{\Gamma^{yy}}{\hbar^2}S_y - \frac{\Gamma^{yx}}{\hbar^2}S_x - \frac{C_y}{\hbar^2} = 0,$$

$$D\frac{\partial^2}{\partial y^2}S_x + \frac{R^{xzy}}{\hbar}\frac{\partial}{\partial y}S_z - \frac{\Gamma^{xx}}{\hbar^2}S_x - \frac{\Gamma^{xy}}{\hbar^2}S_y - \frac{C_x}{\hbar^2} = 0, \tag{2}$$

where diffusion constant $D = v_F^2\tau/2$, and S_i is the spin density in units of $\hbar$. Since $k_F l_e \gg 1$, charge neutrality is maintained by the condition of zero net charge density throughout.

The DP spin-relaxation rates $\Gamma^{il} = 4\tau\overline{h_k^2(\delta^{il} - n_k^i n_k^l)}$ for $i, l \in 1, 2$, and 3, for unit vector $\mathbf{n_k} = \mathbf{h_k}/h_k$. The overline denotes the angular average over the Fermi surface. Specifically, we have $\Gamma^{xx} = \Gamma^{yy} = \Gamma^{zz}/2 = 2\tau k_F^2(\alpha^2 + \tilde{\beta}^2 - \frac{1}{2}\tilde{\beta}^2\tilde{k}^2 + \frac{1}{8}\tilde{\beta}^2\tilde{k}^4)$ and $\Gamma^{xy} = \Gamma^{yx} = -\alpha\tau k_F^2\tilde{\beta}(4 - \tilde{k}^2)$ for $\tilde{k} = k_F/\kappa$. The diagonal components of the DP spin-relaxation rate receive independent contributions from the individual SOI. The off-diagonal DP components, however, involve both SOIs together, as they are proportional to $\alpha\tilde{\beta}$. Furthermore, $\tilde{k}$ serves as an agent that carries the cubic-k effects of the DSOI. For example, the term that has $\tilde{\beta}^2\tilde{k}^2$ is resulted from mixing the linear-k and the cubic-k effects of the DSOI, whereas the term that has $\tilde{\beta}^2\tilde{k}^4$ is due solely to the cubic-k effect of the DSOI, and in its second order.

Spin precession arising from spatial nonuniformity in spin densities is characterized by coefficients $R^{ilm} = 4\tau\Sigma_n \varepsilon^{iln} h_k^n v_F^m$, where ε^{iln} is the Levi-Civita symbol. Specifically, the RSOI's contributions are $R^{yzy} = -R^{zyy} = \frac{2\tau k_F^2}{m^*}\alpha$, and the DSOI's contributions are $R^{zxy} = -R^{xzy} = \frac{2\tau k_F^2}{m^*}(\tilde{\beta} - \frac{1}{4}\tilde{\beta}\tilde{k}^2)$. As we will explore the interplay between the two SOIs by varying α while keeping $\tilde{\beta}$ fixed, it is more convenient to define the length scale $l_{\rm so} = 2D/R^{zxy}$ according to the strength of $\tilde{\beta}$ only. The coefficient R^{ilm}, if not zero, causes the precession of S_l, due to its

spatial variation along $\hat{m}$, to rotate into S_i. That R^{zyy}, for instance, receives sole contribution from RSOI can be understood from our aforementioned shifted electron-distribution picture. Taking that $S_y(q_y)$ is represented by a shifted distribution with $\hat{\mathbf{Q}}=-\hat{\mathbf{y}}$, the effective magnetic field $\mathbf{h}^{\mathbf{R}}$ due to RSOI will be along $\hat{\mathbf{Q}}\times\hat{\mathbf{z}}=-\hat{\mathbf{x}}$, leading to the precession of S_y about $\hat{x}$ clockwise. On the other hand, the effective magnetic field $\mathbf{h}^{\mathbf{D}}$ due to DSOI for this case will be along $-\hat{y}$, assuming low electron-density regime, and cannot lead to the precession of S_y. Similar argument can be applied to explain why R^{zxy}, for instance, receives contribution from DSOI only.

The effect of the driving electric field on the above spin diffusion enters through the coefficients C_i, for $i\in 1,2$. It is given by $C_i=\frac{1}{2}M_x^{i0}\partial D_0^0/\partial x$, where $M_x^{i0}=4\tau^2 h_k^3\frac{\partial n_k^i}{\partial k_x}$ incorporates the spin-charge coupling and $D_0^0=-2N_0eEx$ is a local equilibrium density.[17] The bulk spin densities can be solved directly from Eq. (2). We obtain $S_y^B=\frac{-C_x\Gamma^{yx}+C_y\Gamma^{xx}}{\Gamma^{xy}\Gamma^{yx}-\Gamma^{xx}\Gamma^{yy}}$, $S_x^B=\frac{C_x\Gamma^{yy}-C_y\Gamma^{xy}}{\Gamma^{xy}\Gamma^{yx}-\Gamma^{xx}\Gamma^{yy}}$, and $S_z^B=0$. The full expressions are given by

$$S_x^B=\left(\frac{\tau N_0eE\tilde{\beta}}{2\hbar}\right)\times\frac{(8\alpha^4-16\alpha^2\tilde{\beta}^2+8\tilde{\beta}^4)+(2\alpha^4+8\alpha^2\tilde{\beta}^2-10\tilde{\beta}^4)\tilde{k}^2+(\alpha^2\tilde{\beta}^2+3\tilde{\beta}^4)\tilde{k}^4+\left(-\frac{3}{8}\alpha^2\tilde{\beta}^2+\frac{1}{8}\tilde{\beta}^4\right)\tilde{k}^6-\frac{5}{16}\tilde{\beta}^4\tilde{k}^8+\frac{3}{64}\tilde{\beta}^4\tilde{k}^{10}}{(-4\alpha^4+8\alpha^2\tilde{\beta}^2-4\tilde{\beta}^4)+(-4\alpha^2\tilde{\beta}^2+4\tilde{\beta}^4)\tilde{k}^2-2\tilde{\beta}^4\tilde{k}^4+\frac{1}{2}\tilde{\beta}^4\tilde{k}^6-\frac{1}{16}\tilde{\beta}^4\tilde{k}^8},$$

$$S_y^B=\left(\frac{\tau N_0eE\alpha}{2\hbar}\right)\times\frac{(8\alpha^4-16\alpha^2\tilde{\beta}^2+8\tilde{\beta}^4)+(12\alpha^2\tilde{\beta}^2-12\tilde{\beta}^4)\tilde{k}^2+(\alpha^2\tilde{\beta}^2+3\tilde{\beta}^4)\tilde{k}^4-\frac{1}{4}\tilde{\beta}^4\tilde{k}^6+\frac{3}{16}\tilde{\beta}^4\tilde{k}^8}{(-4\alpha^4+8\alpha^2\tilde{\beta}^2-4\tilde{\beta}^4)+(-4\alpha^2\tilde{\beta}^2+4\tilde{\beta}^4)\tilde{k}^2-2\tilde{\beta}^4\tilde{k}^4+\frac{1}{2}\tilde{\beta}^4\tilde{k}^6-\frac{1}{16}\tilde{\beta}^4\tilde{k}^8}. \quad (3)$$

Equation (3) reduces to the pure RSOI result[3] when $\tilde{\beta}=0$, and to the pure cubic-k DSOI result[17] when $\alpha=0$. If the cubic-k term in the DSOI is dropped ($\tilde{k}=0$), Eq. (3) gives $\mathbf{S}_{\mathrm{LRD}}^B=-\frac{\tau N_0eE}{\hbar}(\tilde{\beta},\alpha)$ so that it points to the third quadrant in the x-y plane. For $\alpha=\tilde{\beta}$, $\mathbf{S}_{\mathrm{LRD}}^B$ forms 45° with the $-x$ axis.

We solve the spin-diffusion equation for the spin density S_i across the semiconductor strip. The boundary condition we use is derived from requiring the local spin-current density I_y^i, which is expressed in terms of both S_i and its spatial derivative $\partial S_i/\partial y$, to be zero in its transverse flow I_y^i at the lateral edges.[17] This is appropriate for a hard-wall boundary.[33,34] Extended to include both SOIs, the spin-current density is given by

$$I_y^z=-2D\frac{\partial}{\partial y}S_z-R^{zyy}(S_y-S_y^B)-R^{zxy}(S_x-S_x^B)+I_{sH}\delta_{iz},$$

$$I_y^y=-2D\frac{\partial}{\partial y}S_y-R^{yzy}S_z,$$

$$I_y^x=-2D\frac{\partial}{\partial y}S_x-R^{xzy}S_z. \quad (4)$$

The spin-current density in Eq. (4) has contribution from spin diffusion, via the spatial gradients in S_i, spin precession, via the R^{ilm} coefficients, and the electric field, via the bulk spin-current density I_{sH}. It is given by

$$I_{sH}=-R^{zyy}S_y^b-R^{zxy}S_x^b+4\tau^2eEN_0v_F^y\overline{\left(\frac{\partial\mathbf{h}_\mathbf{k}}{\partial k_x}\times\mathbf{h}_\mathbf{k}\right)_z}. \quad (5)$$

III. NUMERICAL RESULTS AND DISCUSSIONS

In this section, we present the edge spin accumulation S_z and the bulk spin polarizations $\mathbf{S}^B$ for a 2DEG semiconductor strip that consists of both the RSOI and the cubic-k DSOI. For definiteness, material parameters are chosen to be consistent with GaAs: effective mass $m^*=0.067m_0$, with m_0 the electron mass; *Dresselhaus* SOI $\beta=27.5$ eV Å^3,[32] and $\tilde{\beta}(\equiv\beta\kappa^2)=2.22$ eV m for quantum well thickness $w=300$ Å. The width of the strip is $d=30$ μm, and the mean free path $l_e=1$ μm. Typical value of l_{so} for $n=1\times10^{15}$ m^{-2}, or $\tilde{k}=0.76$, is $l_{\mathrm{so}}=2.20$ μm. The electrons occupy only the lowest subband in the quantum well. An electric field $E=25$ mV/μm is applied along x to set up the spin-Hall phenomenon.

Figure 1 presents the spatial profile of S_z across the semiconductor strip. Besides the well-known odd-parity feature of S_z in the transverse coordinate y, Figs. 1(a)–1(d) show, for the given physical parameter ranges, that the spin accumulation S_z is sensitive to the ratio $\alpha/\tilde{\beta}$. S_z has the largest magnitude in Fig. 1(a), where $\alpha/\tilde{\beta}=0$; it exhibits sign changes in Figs. 1(b) and 1(c), where $\alpha/\tilde{\beta}=0.5$ and 1, respectively; and it is essentially suppressed in Fig. 1(d), when $\alpha/\tilde{\beta}=2.0$. The fact that the RSOI dominates as early as $\alpha/\tilde{\beta}=2.0$ is surprising.

Dependence of S_z on the electron density, or $\tilde{k}$, is also shown in Fig. 1. For the case of pure Dresselhaus SOI, the edge spin accumulation S_z increases with $\tilde{k}$. This feature corroborates with the fact that the cubic-k SOI is the major contributor to S_z. On the other hand, S_z can change sign by either increasing the electron density, as is shown by the $\tilde{k}=1.20$ curve in Fig. 1(b), or by increasing the $\alpha/\tilde{\beta}$ ratio, as is

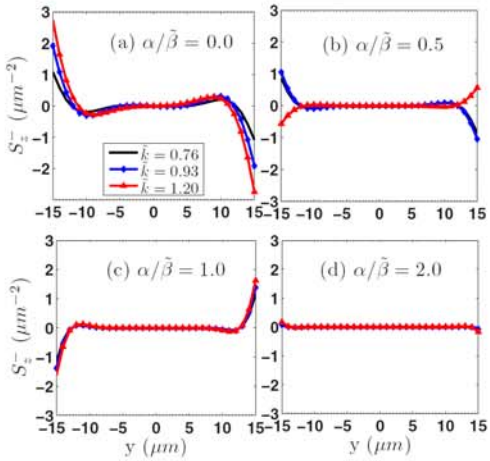

FIG. 1. (Color online) Spatial profile of spin density: S_z versus y. S_z in units of μm^{-2}, y in units of μm, and the width of the strip $d=30$ μm. $\tilde{k}=0.76$ (black solid line), 0.93 (blue diamond), and 1.20 (red triangle) correspond to electron density $n=1.0$, 1.5, and 2.5×10^{15} m^{-2}. The ratio $\alpha/\tilde{\beta}=0.0$, 0.5, 1.0, and 2.0 in (a)–(d), respectively.

shown by the curves in Fig. 1(c). This sign change in S_z is a manifestation of the competition between the RSOI and the cubic-k DSOI. That the RSOI joins forces with the cubic-k DSOI to compete with the pure cubic-k DSOI feature is an intriguing result we have found here. This is supported by Fig. 1(b), when the RSOI is of intermediate strength. The sign change in S_z occurs for the $\tilde{k}=1.20$ curve of which the cubic-k effect is the strongest. For larger RSOI, as in Fig. 1(c), the sign change occurs for all curves shown, including those of smaller $\tilde{k}$ values. All these characteristics, and the results in the following, have prompted us to categorize the spin accumulation into three regimes: the Dresselhaus-dominated regime, Fig. 1(a); the Rashba-dominated regime, Fig. 1(d); and the intermediate regime, Figs. 1(b) and 1(c). The ratio $\alpha/\tilde{\beta}$ is the key parameter that helps define these regimes. We note in passing that we have treated α and $\tilde{k}$ as though they were independent parameters whereas in practice they may be connected. It has been demonstrated experimentally, however, that the two parameters can be decoupled by a two gates technique.[35]

The dependence of the edge spin accumulation $S_z^- \equiv S_z(y=-d/2)$ at the sample edge on the regime parameter $\alpha/\tilde{\beta}$ is presented in Fig. 2. The first feature that we want to address about these curves is their even parity in $\alpha/\tilde{\beta}$. This confirms our expectation nicely because the symmetry of the system seems to demand a parity symmetry in S_z^- with respect to $\alpha/\tilde{\beta}$. However, the fact that $S_z^- \neq 0$ at $\alpha/\tilde{\beta}=0$ rules out the possibility for a S_z^- of odd parity, leaving us the even parity as the only choice. There are other features, which are equally important, in the general dependence of S_z^- on $\alpha/\tilde{\beta}$. Starting from a maximum at $\alpha/\tilde{\beta}=0$, S_z^- passes through a minimum of negative value and then diminishes to small values at $\alpha/\tilde{\beta}=2$. The minima occur within a region $0.5 < \alpha/\tilde{\beta} < 1$. These minima of S_z^- are resulted from the competition between the two SOIs. In contrast, the maximum of S_z^- is a pure DSOI feature. The maximum value of S_z^- increases with $\tilde{k}$ up to around $\tilde{k}=1.20$. Beyond this, the maximum value of S_z^- takes on a different course and decreases with increasing $\tilde{k}$ to negative values, as is indicated by the $\tilde{k}=1.51$ curve. Suppression on S_z^- is already quite significant when $\alpha/\tilde{\beta}>1.5$. On the other hand, taking both directions of S_z^- into account, $|\alpha/\tilde{\beta}|<1$ is the optimal region for the exhibition of spin accumulation.

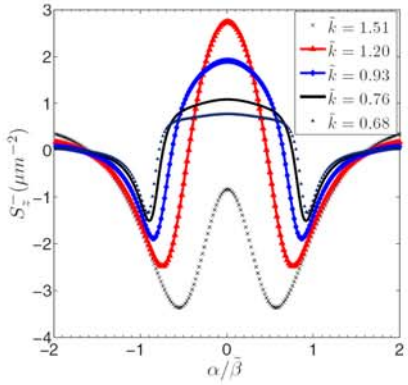

FIG. 2. (Color online) Edge spin accumulation S_z^- versus $\alpha/\tilde{\beta}$. $\tilde{k}=1.51$ (black cross), 1.20 (red triangle), 0.93 (blue diamond), 0.76 (black solid line), and 0.68 (black triangle) correspond to electron density $n=3.5$, 2.5, 1.5, 1.0, and 0.8×10^{15} m^{-2}, respectively. The curves show the symmetry $S_z^-(\alpha)=S_z^-(-\alpha)$.

Presented in Fig. 3 is the dependence of S_z^- on both $\tilde{k}$ and $\alpha/\tilde{\beta}$. It is meant to be a comprehensive presentation, with S_z^- versus $\tilde{k}$ curves plotted together for different values of $\alpha/\tilde{\beta}$ ($0\leq\alpha/\tilde{\beta}\leq2$). The pure DSOI case is denoted by the circular dots and the $\alpha/\tilde{\beta}=1$ case is denoted by the open circles. The $\alpha/\tilde{\beta}=2$ case forms the boundary of the group of curves of increasing M, where the variation in S_z^- with $\tilde{k}$ is weak and the magnitudes small. It is convenient to describe the general features separately in two regions: the $0\leq\alpha/\tilde{\beta}\leq1$ and the $1\leq\alpha/\tilde{\beta}\leq2$ regions. In the former region the S_z^- increases with $\tilde{k}$ initially, following quite closely with the $\alpha/\tilde{\beta}=0$ curve, before it reaches its maximum. Beyond this point, S_z^- deviates from the $\alpha/\tilde{\beta}=0$ curve and decreases to pass through zero and into the negative value region. The increasing of $\alpha/\tilde{\beta}$ results in the negative shifting in the $\tilde{k}$ values of the zero of S_z^-. There is a tendency, as $\tilde{k}$ further increases, for the S_z^- to conform to the pure DSOI behavior, namely, that S_z^- increases its magnitude with $\tilde{k}$. This tendency, however, gradually fades out, for $\alpha/\tilde{\beta}>0.4$, and results in a much weaker dependence on $\tilde{k}$ when $\alpha/\tilde{\beta}\approx2$.

The domination of the pure DSOI in the small $\tilde{k}$ region is consistent with the understanding that the DSOI is the sole contributor to S_z^- there and the effect of RSOI needs to be

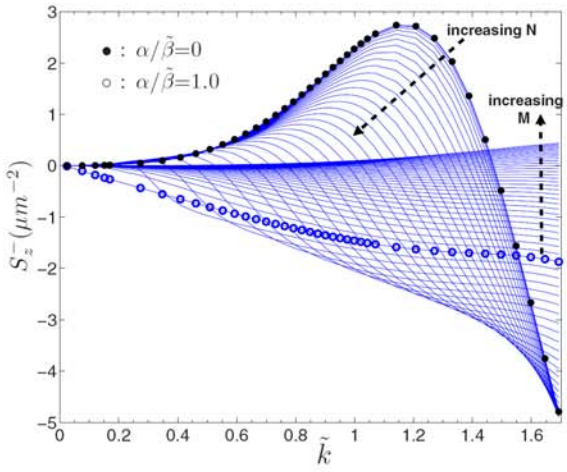

FIG. 3. (Color online) Spin densities S_z^- versus $\tilde{k}$. The case of pure Dresselhaus SOI ($\alpha/\tilde{\beta}=0$) is denoted by black circular dots. The case of $\alpha/\tilde{\beta}=1.0$ is indicated by blue open circles. Intermediate between them we have curves for $\alpha/\tilde{\beta}=N\times\Delta$, where $\Delta=\frac{1}{32}$. From $\alpha/\tilde{\beta}=1$ to $\alpha/\tilde{\beta}=2$ we have curves for $\alpha/\tilde{\beta}=1+M\times\Delta$. S_z^- is essentially suppressed when $\alpha\approx 2\tilde{\beta}$.

mediated by the cubic-k DSOI. The effects of RSOI emerge in larger $\tilde{k}$ values, where the location of the zero of S_z^- is negatively shifted with the increasing of $\alpha/\tilde{\beta}$. The zero of S_z^- can be understood with the vanishing of the effective magnetic field $\mathbf{h}=0$. Taking the $\alpha/\tilde{\beta}=0$ case as an example, $\langle\mathbf{h}^D\rangle=\langle[k_x(-\tilde{\beta}+\beta k_y^2),k_y(\tilde{\beta}-\beta k_x^2)]\rangle$. In a driving $\mathbf{E}$ field, the averages $\langle k_x\rangle=-\tau e/\hbar\mathbf{E}$ and $\langle k_y\rangle=0$ so that $\langle\mathbf{h}^D\rangle$ becomes zero if $\langle\tilde{\beta}-\beta k_y^2\rangle=0$. This condition is satisfied if $\tilde{k}=\sqrt{2}$, which is quite close to the value $\tilde{k}=1.47$ for the pure DSOI curve. We point out that the averages on $\mathbf{h}$ that enter into the contribution to the various processes considered in this work are much complicated than the one that we have just shown. But this nice correspondence in the $\tilde{k}$ values for the $\alpha/\tilde{\beta}=0$ case convinces us that the effective magnetic field concept is at work. This effect of α on the zero of S_z^- shows that the effect of RSOI is a competing one. Similar competing nature causes the suppression of the pure DSOI feature in the $\tilde{k}>1.2$ region. As is demonstrated by the $\alpha/\tilde{\beta}=1$ curve, the pure DSOI trend in this region no longer prevails but is largely suppressed. It is also of interest to see that S_z^- is negative in the entire shown values of $\tilde{k}$.

For the $1\leq\alpha/\tilde{\beta}\leq 2$ region, S_z^- decreases monotonically in its magnitude with the increasing of $\alpha/\tilde{\beta}$, while exhibiting a converging behavior as $\alpha/\tilde{\beta}$ increases. Except for a residual positive value for S_z^- in the large $\tilde{k}$ region when $\alpha/\tilde{\beta}=2$, the S_z^- is essentially suppressed.

In Figs. 4 and 5 we present both the bulk spin polarization $\mathbf{S}^B$ and its linear-k counterpart $\mathbf{S}^B_{\mathrm{LRD}}$ and their dependence on $\alpha/\tilde{\beta}$ and $\tilde{k}$. Relative magnitude between each vector pairs is shown, with the magnitude of $\mathbf{S}^B_{\mathrm{LRD}}$ chosen as unity. For a

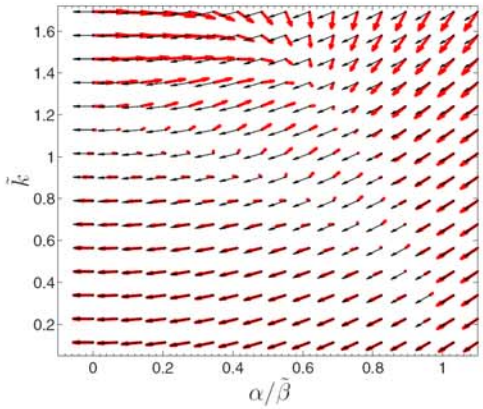

FIG. 4. (Color online) Bulk spin polarization $\mathbf{S}^B$ as a function of $\alpha/\tilde{\beta}$ (abscissa) and $\tilde{k}$ (ordinate), and for $0\leq\alpha/\tilde{\beta}\leq 1.2$. Directions of $\mathbf{S}^B$ are shown with x and y axes along the abscissa axis (pointing right) and the ordinate axis (pointing upward), respectively. $\mathbf{S}^B_{\mathrm{LRD}}$ (black arrows) denotes the linear-k SOIs, and $\mathbf{S}^B$ (red diffused arrows) denotes the full SOIs. The magnitudes of the vector pairs are normalized between themselves such that the magnitude of the bulk spin polarization is $|\mathbf{S}^B|/|\mathbf{S}^B_{\mathrm{LRD}}|$, and that of $\mathbf{S}^B_{\mathrm{LRD}}$ is unity.

fixed $\tilde{k}$, the two vector pairs become more aligned in both their directions and magnitudes when $\alpha/\tilde{\beta}$ increases. For a fixed $\alpha/\tilde{\beta}$ the general feature is that the vector pairs deviate more from each other as $\tilde{k}$ increases. This is consistent with the understanding that the deviation comes from the cubic k in the DSOI. There is an interesting intermediate region where the $\mathbf{S}^B\approx 0$. Starting from $\alpha/\tilde{\beta}=0$, the zero S^B is around $\tilde{k}\approx 1.1$. With the increasing of $\alpha/\tilde{\beta}$, the $\tilde{k}$ value for zero S^B decreases. This zero S^B feature ties up nicely with the zero S_z^- feature in Fig. 3 in that both of the $\tilde{k}$ values for the corresponding zeros decrease with the increasing of $\alpha/\tilde{\beta}$. Beyond the region $\alpha/\tilde{\beta}\geq 1$, the zero S^B feature subsides while the vector pairs align nicely with each other, both in

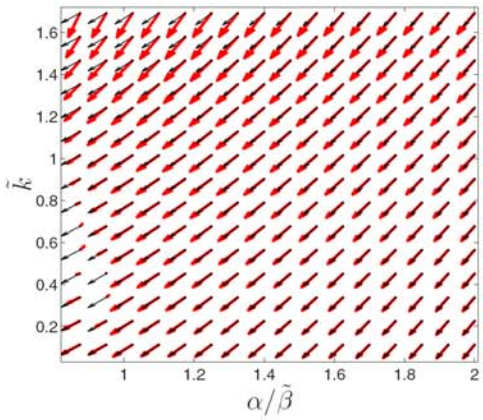

FIG. 5. (Color online) Bulk spin polarization $\mathbf{S}^B$ as a function of $\alpha/\tilde{\beta}$ and $\tilde{k}$, and for $0.9\leq\alpha/\tilde{\beta}\leq 2.0$.

direction and magnitude, unless for very large $\tilde{k}$. Thus the RSOI helps to make the linear-k SOI dominates in the formation of S^B for $\alpha/\tilde{\beta}>1$.

IV. CONCLUSION

In conclusion, we have studied systematically the competing interplay between the RSOI and the cubic-k DSOI in their contribution to the edge spin accumulation and the bulk spin polarization. There are three regimes, namely, the Dresselhaus-dominated regime ($|\alpha/\tilde{\beta}|<0.5$); the Rashba-dominated regime ($|\alpha/\tilde{\beta}|\approx 2$); and the intermediate regime ($0.5<|\alpha/\tilde{\beta}|\approx 1$). The optimal restoration of the spin accumulation occurs in the region $|\alpha/\tilde{\beta}|<1.0$. While the RSOI alone cannot give rise to spin accumulation, it can still exert its effect via the cubic-k DSOI, and thus provide the needed tunability for spin accumulations.

ACKNOWLEDGMENTS

This work was supported by Taiwan NSC (Contract No. 96-2112-M-009-0038-MY3), NCTS Taiwan, Russian RFBR (Contract No. 060216699), and a MOE-ATU grant.

[1] M. I. Dyakonov and V. I. Perel, Phys. Lett. **35A**, 459 (1971).
[2] A. A. Bakun, B. P. Zakharchenya, A. A. Rogachev, M. N. Tkachuk, and V. G. Fleisher, JETP Lett. **40**, 1293 (1984).
[3] V. M. Edelstein, Solid State Commun. **73**, 233 (1990).
[4] A. G. Aronov, Yu. B. Lyanda-Geller, and G. E. Pikus, Sov. Phys. JETP **73**, 537 (1991).
[5] J. E. Hirsch, Phys. Rev. Lett. **83**, 1834 (1999).
[6] S. Murakami, N. Nagaosa, and S. C. Zhang, Science **301**, 1348 (2003).
[7] J. Sinova, D. Culcer, Q. Niu, N. A. Sinitsyn, T. Jungwirth, and A. H. MacDonald, Phys. Rev. Lett. **92**, 126603 (2004).
[8] Y. K. Kato, R. C. Myers, A. C. Gossard, and D. D. Awschalom, Science **306**, 1910 (2004).
[9] J. Wunderlich, B. Kaestner, J. Sinova, and T. Jungwirth, Phys. Rev. Lett. **94**, 047204 (2005).
[10] E. I. Rashba, Sov. Phys. Solid State **2**, 1109 (1960); Yu. A. Bychkov and E. I. Rashba, JETP Lett. **39**, 78 (1984).
[11] H. A. Engel, B. I. Halperin, and E. I. Rashba, Phys. Rev. Lett. **95**, 166605 (2005).
[12] H. A. Engel, E. I. Rashba, and B. I. Halperin, Phys. Rev. Lett. **98**, 036602 (2007).
[13] G. Dresselhaus, Phys. Rev. **100**, 580 (1955).
[14] A. G. Mal'shukov and K. A. Chao, Phys. Rev. B **71**, 121308(R) (2005).
[15] J. I. Inoue, G. E. W. Bauer, and L. W. Molenkamp, Phys. Rev. B **70**, 041303(R) (2004); E. G. Mishchenko, A. V. Shytov, and B. I. Halperin, Phys. Rev. Lett. **93**, 226602 (2004); A. A. Burkov, A. S. Núñez, and A. H. MacDonald, Phys. Rev. B **70**, 155308 (2004); R. Raimondi and P. Schwab, *ibid.* **71**, 033311 (2005); O. V. Dimitrova, *ibid.* **71**, 245327 (2005).
[16] B. A. Bernevig and S. C. Zhang, Phys. Rev. Lett. **95**, 016801 (2005).
[17] A. G. Mal'shukov, L. Y. Wang, C. S. Chu, and K. A. Chao, Phys. Rev. Lett. **95**, 146601 (2005).
[18] F. G. Pikus and G. E. Pikus, Phys. Rev. B **51**, 16928 (1995).
[19] J. Schliemann, J. C. Egues, and D. Loss, Phys. Rev. Lett. **90**, 146801 (2003).
[20] X. Cartoixà, D. Z.-Y. Ting, and Y.-C. Chang, Appl. Phys. Lett. **83**, 1462 (2003).
[21] J. B. Miller, D. M. Zumbühl, C. M. Marcus, Y. B. Lyanda-Geller, D. Goldhaber-Gordon, K. Campman, and A. C. Gossard, Phys. Rev. Lett. **90**, 076807 (2003).
[22] S. D. Ganichev, V. V. Bel'kov, L. E. Golub, E. L. Ivchenko, P. Schneider, S. Giglberger, J. Eroms, J. De Boeck, G. Borghs, W. Wegscheider, D. Weiss, and W. Prettl, Phys. Rev. Lett. **92**, 256601 (2004).
[23] S. Q. Shen, Phys. Rev. B **70**, 081311(R) (2004).
[24] B. A. Bernevig, J. Orenstein, and S. C. Zhang, Phys. Rev. Lett. **97**, 236601 (2006).
[25] M. H. Liu, K. W. Chen, S. H. Chen, and C. R. Chang, Phys. Rev. B **74**, 235322 (2006).
[26] L. Meier, G. Salis, I. Shorubalko, E. Gini, S. Schön, and K. Ensslin, Nat. Phys. **3**, 650 (2007).
[27] S. Giglberger, L. E. Golub, V. V. Bel'kov, S. N. Danilov, D. Schuh, C. Gerl, F. Rohlfing, J. Stahl, W. Wegscheider, D. Weiss, W. Prettl, and S. D. Ganichev, Phys. Rev. B **75**, 035327 (2007).
[28] M. Scheid, M. Kohda, Y. Kunihashi, K. Richter, and J. Nitta, Phys. Rev. Lett. **101**, 266401 (2008).
[29] M. Wang, K. Chang, and K. S. Chan, Appl. Phys. Lett. **94**, 052108 (2009).
[30] A. A. Abrikosov, L. P. Gorkov, and I. E. Dzyaloshinskii, *Method of Quantum Field Theory in Statistical Physics* (Dover, New York, 1975).
[31] L. Y. Wang, C. S. Chu, and A. G. Mal'shukov, Phys. Rev. B **78**, 155302 (2008).
[32] R. Winkler, *Spin-Orbit Coupling Effects in Two-Dimensional Electron and Hole Systems*, (Springer-Verlag, Berlin, 2003).
[33] O. Bleibaum, Phys. Rev. B **74**, 113309 (2006).
[34] Y. Tserkovnyak, B. I. Halperin, A. A. Kovalev, and A. Brataas, Phys. Rev. B **76**, 085319 (2007).
[35] D. Grundler, Phys. Rev. Lett. **84**, 6074 (2000).

Appendix B:

PHYSICAL REVIEW B **78**, 155302 (2008)

Asymmetries in intrinsic spin-Hall effect in low in-plane magnetic field

L. Y. Wang,[1] C. S. Chu,[1,2] and A. G. Mal'shukov[1,2,3]
[1]*Department of Electrophysics, National Chiao Tung University, Hsinchu 30010, Taiwan*
[2]*Physics Division, National Center for Theoretical Sciences, Hsinchu 30043, Taiwan*
[3]*Institute of Spectroscopy, Russian Academy of Science, 142190 Troitsk, Moscow oblast, Russia*
(Received 22 June 2008; revised manuscript received 2 September 2008; published 2 October 2008)

Effects of low in-plane magnetic field on bulk spin densities and edge spin accumulations of a diffusive two-dimensional semiconductor stripe are studied. Focusing upon the Dresselhaus-type intrinsic spin-orbit interaction (SOI), we look for the symmetry, or asymmetry, characteristics in two magnetic-field orientations: along and transverse to the stripe. For longitudinal field, the out-of-plane spin density S_z exhibits odd parity across the stripe and even parity in the magnetic field and is an edge accumulation. For transverse field, the out-of-plane S_z becomes asymmetric in both spatial and field dependencies and has finite bulk values for finite magnetic fields. Our results support utilizing low in-plane magnetic fields for the probing of the underlying SOI.

DOI: 10.1103/PhysRevB.78.155302 PACS number(s): 72.25.Dc, 71.70.Ej, 73.40.Lq

I. INTRODUCTION

Generation and manipulation of spin densities by electrical means are major goals of semiconductor spintronics that are made possible by spin-orbit interactions (SOI).[1–8] SOIs being considered are either intrinsiclike: the Rashba[2,5,7,9–11] and the Dresselhaus SOIs[4,8,12,13] or extrinsiclike: the impurity-induced SOI.[1,3,6,10,14] These SOIs contribute, in an external electric field, to either spin densities in the bulk or spin accumulations at lateral edges, or both.

Out-of-plane spin polarization is of particular interest because it permits efficient optical probe by Kerr rotation. The edge spin accumulation, according to the spin-Hall effect (SHE), has an out-of-plane component and is resulted from a transverse spin current induced by the electric field.[1,4–6] However, for the case of intrinsic SOI, it is understood that the SHE is quenched by background scatterers, be they isotropic or anisotropic,[15] as long as the intrinsic SOIs consist of only linear-momentum dependence term. Meanwhile, no out-of-plane bulk spin densities are expected in an electric field.[2,10,16] When applying an in-plane magnetic field to a two-dimensional (2D) system, one might be led by the in-plane nature of the effective spin-orbit magnetic field $\mathbf{h}_{\text{eff}} = \langle \mathbf{h}_{\mathbf{k}} \rangle \neq 0$, obtained by averaging the spin-orbit effective field over the distribution of the electron momentum $\hbar\mathbf{k}$, to expect that there were no out-of-plane spin densities. This is shown not to be the case by Engel *et al.*[11] for a Rashba-type 2D system, where out-of-plane spin densities are found when the external in-plane magnetic field is longitudinal: a configuration studied by recent experiments.[17,18] However, either the scatterer has to be anisotropic or the electron dispersion has to be nonparabolic for the effect to hold.[11] Here, longitudinal denotes the direction parallel to the electric field and its orthogonal counterpart in the 2D plane is denoted transverse.

In this paper, we have shown that out-of-plane bulk spin density can be generated in another system configuration with less restrictive assumptions. The configuration is a Dresselhaus-type 2D system and the external in-plane magnetic field is in a transverse orientation. More importantly, the effect holds for isotropic background scatterers and for parabolic dispersion for electrons. Our calculation has included the cubic Dresselhaus SOI.

This paper also addresses the symmetrical properties of the spin densities and spin accumulations in a weak in-plane magnetic field. We believe that this is important for distinguishing the dominant type of SOI in a particular sample. Out-of-plane spin accumulations at the lateral edges of an extrinsic SOI two-dimensional electron gas (2DEG) are symmetric with respect to a transverse magnetic field.[6] The suppression that it exerts on the spin accumulations is exhibited in the position-dependent Hanle profiles.[19] Study on the same field configuration, but in an extrinsic SOI normal metal, has found similar field suppression in another physical quantity: the out-of-plane spin-Hall potential.[20] For the intrinsic SOI, studies on the in-plane magnetic-field effects have focused on the spin-Hall conductivity[21,22] and the bulk spin densities[11,23] but not on the symmetry properties. Thus it is legitimate to perform a thorough and systematic investigation on both the spatial as well as the field-dependent symmetry characteristics of the spin distributions for the case of intrinsic SOI.

Our results show, for the case of a Dresselhaus-type 2DEG stripe, strong anisotropy in the symmetry characteristics with respect to the field orientations. For longitudinal field, the out-of-plane spin density S_z exhibits odd parity across the stripe and even parity in the magnetic field and is an edge accumulation. For transverse field, S_z becomes asymmetric in both spatial and field dependencies and has finite bulk values for finite magnetic fields. As the Rashba and the extrinsic SOIs do not depend on the crystal orientations, while the Dresselhaus SOI does, the strong anisotropy in the symmetry characteristics obtained in this work is distinct for the Dresselhaus SOI. Our work thus serves to commence the notion of utilizing low in-plane magnetic fields as a characterizing tool for the probing of the underlying SOI in a particular sample.

In this paper, we consider a diffusive Dresselhaus-type 2DEG stripe in a weak in-plane magnetic field as shown in Fig. 1. The diffusive regime has $l_{so} \gg l_e$, where l_{so} and l_e are, respectively, the spin-relaxation length due to the SOI and

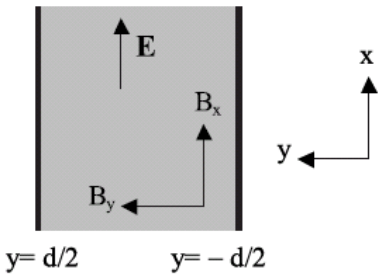

FIG. 1. Top-view schematic illustration of the 2D stripe. The 2D stripe has a width d. In the system, electric field $\mathbf{E}$ and in-plane magnetic field $\mathbf{B}$ are applied. The direction along the stripe, or $\hat{x}$, is denoted longitudinal and that along $\hat{y}$, transverse.

momentum relaxation length. Spin distributions across the entire width of the stripe are investigated for all three spin directions including out-of-plane and in-plane components. In Sec. II we present the spin-diffusion equation and the associated boundary conditions. In Sec. III, we present our numerical results. Finally, in Sec. IV, we will present a summary and discussion of our results.

II. SPIN-DIFFUSION EQUATION

Following on the procedure of deriving the spin-diffusion equation for $\mathbf{B}=0$ from the Keldysh nonequilibrium Green's function technique,[16] we extend the derivation to include an in-plane magnetic field. The spin-dependent term in the Hamiltonian is given by $\mathbf{H}_B\cdot\boldsymbol{\sigma}=(\mathbf{h}_\mathbf{k}+\tilde{\mathbf{B}})\cdot\boldsymbol{\sigma}$, where $\boldsymbol{\sigma}$ is the Pauli-matrix vector, $\mathbf{h}_\mathbf{k}=-\mathbf{h}_{-\mathbf{k}}$ is the SOI effective field and a function of the 2D wave vector $\mathbf{k}$, and $\tilde{\mathbf{B}}=g^*\mu_B\mathbf{B}/2$ is the Zeeman term. Here g^* is the effective g factor and μ_B is the Bohr magneton. We consider the weak magnetic-field regime where $E_\mathrm{F}\gg h_k>\tilde{B}$.

A brief outline of the derivation is presented below. Starting with the perturbation from a four potential given by $H'=\Sigma_i\Phi_i(\mathbf{r},t)\tau^i$, where the 2×2 matrices $\tau^0=1$ and $\tau^{x,y,z}=\sigma_{x,y,z}$ and the four densities $D_i(\mathbf{r},t)=-i\,\mathrm{Tr}[\tau^iG^{-+}(\mathbf{r},\mathbf{r},t,t)]$ are expressed in terms of the full Green's function. Within the linear-response regime, and for $\omega\ll E_\mathrm{F}$, it becomes

$$\mathbf{D}_i(\mathbf{r},\omega)=\int d^2r'\sum_j\Pi_{ij}(\mathbf{r},\mathbf{r}',\omega)\Phi_j(\mathbf{r}',\omega)+\mathbf{D}_i^0(\mathbf{r},\omega). \quad (1)$$

With $2N_0$, the electron density of states $\mathbf{D}_i^0(\mathbf{q},\omega)=-2N_0\Phi_i(\mathbf{q},\omega)$ are easily understood as the local equilibrium densities.[16] This term turns out to be the driving term for the spin-Hall effect; and within the linear response, it suffices to neglect the correction due to $\mathbf{H}_B\cdot\boldsymbol{\sigma}$ in $\mathbf{D}_i^0$.

The response function in the k representation is

$$\Pi_{ij}(\mathbf{q},\omega)=i\omega\sum_{\mathbf{p}_1\mathbf{k}_1}\int\frac{d\omega'}{2\pi}\frac{\partial f_\mathrm{FD}(\omega')}{\partial\omega'}\langle\mathrm{Tr}[G^a(\mathbf{k}_1,\mathbf{p}_1-\mathbf{q},\omega)\times\tau^iG^r(\mathbf{p}_1,\mathbf{k}_1+\mathbf{q},\omega+\omega')\tau^j]\rangle, \quad (2)$$

where $f_\mathrm{FD}(\omega')$ is the Fermi-Dirac distribution function at energy ω' and the angular brackets denote averaging over the random impurity configurations. The averaged Green's function is given by $G^{r(0)}(\mathbf{p},\omega)=1/(\omega-E_\mathbf{p}-\mathbf{H}_B\cdot\boldsymbol{\sigma}+i\Gamma)$, where E_F is the Fermi energy and $\Gamma=1/2\tau$. In the following, we consider the regime $E_\mathrm{F}\gg\Gamma>h_k$. Evaluating Eq. (2) within the ladder series[24] leads to the summation, up to all orders, of a basic diagram $\Psi^{\alpha\gamma}_{\mu\lambda}(\omega,\omega',\mathbf{q})=\frac{c_i}{V}|V_\mathrm{sc}|^2\Sigma_\mathbf{p}G^r_{\gamma\alpha}(\mathbf{p},\omega+\omega')G^a_{\mu\lambda}(\mathbf{p}-\mathbf{q},\omega')$. The response function becomes

$$\Pi_{ij}(\mathbf{q},\omega)=\frac{i\omega}{2\pi}\sum_j\int d\omega'\frac{\partial f_\mathrm{FD}}{\partial\omega'}\left(\frac{\pi N_0}{\Gamma}\right)\tau^j_{\mu\alpha}\tau^j_{\beta\nu}\Psi^{\alpha\gamma}_{\mu\lambda}(\omega,\omega',\mathbf{q})\times\{[1-\Psi(\omega,\omega',\mathbf{q})]^{-1}\}^{\gamma\beta}_{\lambda\nu}, \quad (3)$$

where $1^{\gamma\beta}_{\lambda\nu}\equiv\delta_{\gamma\beta}\delta_{\lambda\nu}$ and $\Gamma/(\pi N_0)=c_i|V_\mathrm{sc}|^2/V$. Here, V is total area of the sample and c_i and V_sc are, respectively, the impurity density and the Fourier transform of a short-range impurity potential at $\mathbf{q}=0$. Making use of the transformation $\Psi^{\gamma\gamma'}_{\lambda\lambda'}=(1/2)\Sigma_{ij}\tau^j_{\gamma\lambda}\Psi^{ij}\tau^j_{\lambda'\gamma'}$, Eqs. (1) and (3) together gives

$$(1-\Psi)^{il}(\mathbf{D}_l-\mathbf{D}_l^0)=i\omega\tau\Psi^{il}\mathbf{D}_l^0, \quad (4)$$

where

$$\Psi^{il}=\frac{\Gamma}{2\pi N_0}\sum_{\mathbf{p}'}\mathrm{Tr}[\tau^iG^{r(0)}(\mathbf{p}',\omega+\omega')\tau^jG^{a(0)}(\mathbf{p}'-\mathbf{q},\omega')]. \quad (5)$$

The charge neutrality is maintained by the condition $D_0=0$, since $E_\mathrm{F}\tau\gg1$ and $\omega=0$.

The spin-diffusion equation can be obtained by expanding Ψ^{il} in lower orders of $\mathbf{q}$ and then by obtaining the Fourier transform of Eq. (4) to the position representation. Expanding Ψ^{il} up to lower orders in h_k and to first order in $\tilde{B}$ results in a total of five terms given by

$$\Psi^{il}=\sum_{\nu=1}^5\Psi^{il}_\nu, \quad (6)$$

where $\mathbf{q}$ and ω dependences are not shown.

The term $\Psi^{il}_1=(1+i\omega\tau-D\tau\mathbf{q}^2)\delta_{il}$ with $D=v_\mathrm{F}^2\tau/2$ produces the regular diffusion equation. The second term $\Psi^{i'l}_2=iq_m\tau R^{i'lm}$, where $R^{ilm}=4\tau\Sigma_n\varepsilon^{iln}\overline{h_k^nv_\mathrm{F}^m}$ and ε^{iln} as the Levi-Civita symbol, causes the spin densities to precess about its local variations. The overline denotes the angular average over the Fermi surface and m,n are the component indices. The third term $\Psi^{il}_3=-\tau\Gamma^{il}$, where $\Gamma^{il}=4\tau\overline{h_k^2(\delta^{il}-n_k^in_k^l)}$ for $i,l\neq0$, and for unit vector $\mathbf{n}_\mathbf{k}=\mathbf{h}_\mathbf{k}/h_k$, describes the Dyakonov-Perel' spin relaxation.[1] The last two terms contain new contributions from the in-plane magnetic fields. In the fourth term, we have $\Psi^{il}_4=\tau R^{ilm}_B$, where $R^{ilm}_B=-\Sigma_m2\varepsilon^{ilm}\tilde{B}_m$ and m is the field component index. This gives rise to precession of the spin densities about the magnetic field. In the fifth term we have the spin-charge coupling $\Psi^{i'0}_5=(-iq)(M^{i'0}_B-M^{i'0})$. Here $M^{i0}=4\tau^3\overline{h_k^3\frac{\partial n_\mathbf{k}^i}{\partial\mathbf{k}}}$ and $M^{i0}_B=2\tau^2(\tilde{B}_x\overline{\frac{\partial h_\mathbf{k}^i}{\partial\mathbf{k}}}-\tilde{B}_y\overline{\frac{\partial h_\mathbf{k}^i}{\partial\mathbf{k}}})\delta_{iz}$. The latter contains the effect of the in-plane magnetic field. Up to this point we have kept a

generic form of the SOI. Applying to the case of Rashba SOI, when $\mathbf{h}_k=\alpha\mathbf{k}\times\hat{z}$, we find no out-of-plane bulk spin densities and no edge spin accumulations, which is consistent with previous findings.[11] A more interesting case is the Dresselhaus SOI, where $\mathbf{h}_k=\beta[k_x(k_y^2-\kappa^2),k_y(\kappa^2-k_x^2)]$.[25] Here $\kappa^2=\langle k_z^2\rangle$ is the average over the thickness of the 2DEG and $\langle h_k^z\rangle=0$. From Eqs. (4) and (6) and the form of h_k, we obtain the static spin-diffusion equations

$$\begin{cases} D\dfrac{\partial^2}{\partial y^2}S_x+\dfrac{R^{xzy}}{\hbar}\dfrac{\partial}{\partial y}S_z-\dfrac{\Gamma^{xx}}{\hbar^2}S_x+\dfrac{2}{\hbar}\tilde{B}_yS_z-\dfrac{C_1}{\hbar^2}=0, \\ D\dfrac{\partial^2}{\partial y^2}S_y-\dfrac{\Gamma^{yy}}{\hbar^2}S_y-\dfrac{2}{\hbar}\tilde{B}_xS_z=0, \\ D\dfrac{\partial^2}{\partial y^2}S_z+\dfrac{R^{zxy}}{\hbar}\dfrac{\partial}{\partial y}S_x-\dfrac{\Gamma^{zz}}{\hbar^2}S_z-\dfrac{2}{\hbar}\tilde{B}_yS_x+\dfrac{2}{\hbar}\tilde{B}_xS_y-\dfrac{\tilde{B}_y}{\hbar}C_2=0, \end{cases} \tag{7}$$

where $S_i=D_i/2$ and the homogeneity along x is assumed. Effects of the in-plane magnetic field enter Eqs. (7) in two places. The first is the precession effect given exactly by $d\boldsymbol{\sigma}/dt=(2/\hbar)\tilde{\mathbf{B}}\times\boldsymbol{\sigma}$. The second is through the coefficient C_2, which is originated from the spin-charge coupling term M_B^{i0}. Its expression is given by $C_2=\tau\overline{(\partial h_k^x/\partial k_x)}(\partial D_0^0/\partial x)$, where $D_0^0=-2N_0eEx$ for $e>0$ represents the effects of the driving electric field.

Expressions for other coefficients in Eqs. (7) are the Dyakonov-Perel' spin relaxation rates $\Gamma^{xx}=\Gamma^{yy}=\Gamma^{zz}/2=\beta^2\tau k_F^6(1/4-C^2+2C^4)$, where $C=\kappa/k_F$. Precessions about local variation in spin densities are given by the coefficients $R^{zxy}=-R^{xzy}=\frac{\beta\pi k_F^4}{m^*}(2C^2-1/2)=2D/l_{so}$. Finally, the spin-charge coupling that originates from M^{i0} is the coefficient $C_1=M^{x0}D_0^0/2$.

The bulk spin densities obtained from Eqs. (7) are

$$\begin{cases} S_z^b=\Lambda_y\left(-\dfrac{1}{2}C_2+\dfrac{C_1}{\Gamma^{xx}}\right)\Big/(1+2\Lambda_x^2+2\Lambda_y^2), \\ S_y^b=-2\Lambda_xS_z^b, \\ S_x^b=2\Lambda_yS_z^b-\dfrac{C_1}{\Gamma^{xx}}, \end{cases} \tag{8}$$

where $\boldsymbol{\Lambda}$, the dimensionless $\tilde{\mathbf{B}}$, is given by $\Lambda_i=\tilde{B}_i/\Gamma^{xx}$. S^b is checked to reproduce the correct $\mathbf{B}=0$ limit.[16] Except for the Λ_yC_2 term in S_z^b, which is originated from the spin-charge coupling, all other terms in S^b that are proportional to Λ_i are related to spin precessions about $\tilde{\mathbf{B}}$.

The boundary condition for the spin-diffusion equation is established in the following by connecting the spin current to the spin densities and their spatial gradients and then requires the transverse flow of the spin current to be zero at the lateral edges.[16] This is appropriate for hard wall boundary.[26,27] We start from the conventional form of the spin current operator $J_l^i\equiv(1/2)(V_l\sigma_i+\sigma_iV_l)$, where spin unit of $\hbar/2$ is implied. The velocity operator is given by

$$V_l\equiv\frac{k_l}{m*}+\frac{\partial\mathbf{h}_\mathbf{k}\cdot\boldsymbol{\sigma}}{\partial k_l}, \tag{9}$$

where $v_l=(k_l/m^*)$. The expression for the spin current is[16]

$$I_l^i(\mathbf{q},\omega)=i\omega\int\frac{d\omega'}{2\pi}\frac{dN_F}{d\omega'}\sum_{\mathbf{k},\mathbf{k}'}\left\langle\left(v_l\sigma_i+\frac{\partial h_\mathbf{k}^i}{\partial k^l}\right)\times G^r\left(\mathbf{k}+\frac{\mathbf{q}}{2},\mathbf{k}'+\frac{\mathbf{q}}{2},\omega+\omega'\right)\tau^j\times G^a\left(\mathbf{k}'-\frac{\mathbf{q}}{2},\mathbf{k}-\frac{\mathbf{q}}{2},\omega'\right)\right\rangle\Phi_j(\mathbf{q},\omega), \tag{10}$$

where the summation convention for repeated indices is adopted. In the dc limit ($\omega=0$) and at zero temperature ($\omega'=E_F$), the spin current is related to the four densities in the form

$$I_l^i=\frac{1}{m^*}[X_l^{ij'}D_{j'}-X_l^{i0}D_0^0+Y_l^{ij'}D_{j'}-Y_l^{i0}D_0^0], \tag{11}$$

where j' denotes the spin indices. The operators to the spin densities are

$$X_l^{ij}\equiv\left(\frac{\Gamma}{2\pi N_0}\right)\sum_\mathbf{k}k_l\times\mathrm{Tr}\left[\tau^jG^{r(0)}\left(\mathbf{k}+\frac{\mathbf{q}}{2},\omega+E_F\right)\tau^iG^{a(0)}\left(\mathbf{k}-\frac{\mathbf{q}}{2},E_F\right)\right], \tag{12}$$

and

$$Y_l^{ij} \equiv \left(\frac{\Gamma}{2\pi N_0}\right)\sum_{\mathbf{k}} \frac{\partial h_k^i}{\partial k_l} \times \mathrm{Tr}\left[G^{r(0)}\left(\mathbf{k}+\frac{\mathbf{q}}{2},\omega+E_F\right)\tau^j G^{a(0)}\left(\mathbf{k}-\frac{\mathbf{q}}{2},E_F\right)\right]. \quad (13)$$

Specifying to the flow of spin along y, we calculate X_y^{ij} and Y_y^{ij} to give

$$X_y^{ij} = -m^*\left(iq_y D\delta_{ij} + \frac{1}{2}R^{ijy}(\delta_{iz}+\delta_{jz})\right) - 2iq_x m^*\tau^2 v_F^y\overline{\left(\mathbf{h}_\mathbf{k}\times\frac{\partial \mathbf{h}_\mathbf{k}}{\partial k_x}\right)_z}\delta_{iz}\delta_{j0} - \overline{\frac{\partial h_k^i}{\partial k_y}}\delta_{j0}, \quad (14)$$

and

$$Y_y^{ij} = \overline{\frac{\partial h_k^i}{\partial k_y}}\delta_{j0}, \quad (15)$$

with the latter being exactly canceled by a term in Eq. (14). Finally, substituting Eqs. (13) and (14) into Eq. (10), we arrive at the spin current expression that provides us the boundary condition $I_y^i=0$ at the lateral edges for the spin-diffusion equation with

$$I_y^i(\mathbf{r}) = -2D\frac{\partial S_i}{\partial y} - \frac{R^{ijy}}{\hbar}(S_j - S_j^b) + \frac{I_{sH}}{\hbar}\delta_{iz}. \quad (16)$$

The first term of I_y^i describes the spin diffusion due to spatial variation in S_i, the second term is the spin precession prompted by the SOI, and $I_{sH}\delta_{iz}$ is the bulk spin current with

$$I_{sH} = -R^{zjy}S_j^b + 4\tau^2 eEN_0 v_F^y\overline{\left(\frac{\partial \mathbf{h}_\mathbf{k}}{\partial k_x}\times\mathbf{h}_\mathbf{k}\right)_z}. \quad (17)$$

Equations (16) and (17) appear to be the same as their counterparts for the $\mathbf{B}=0$ case;[16] but the magnetic field contributes, in its lowest order, via the spin density S_j^b in Eq. (8). It is worth pointing out here that the primary purpose of deriving Eq. (17) is to apply it to a region within a distance much less than l_{so} from the sample boundary. As such, the effect of spin torque[28,29] on the boundary condition should be of secondary importance, and the results in this work should also remain intact. An eventual exploration on this issue, however, is left for future study.

III. NUMERICAL RESULTS: IN-PLANE B FIELD IN A DRESSELHAUS 2D STRIPE

In this section, we present the electric-field-induced bulk spin densities and edge spin accumulations in a Dresselhaus-type 2DEG stripe acted upon by an in-plane magnetic field. Symmetries, or asymmetries, of the spin distributions with respect to spatial coordinates and the magnetic field are presented in two field orientations: longitudinal and transverse.

For definiteness, we use material parameters consistent with GaAs: effective mass $m^*=0.067m_0$, with m_0 the electron mass; effective g factor $g^*=0.44$ (Ref. 30); and the *Dresselhaus* SOI $\beta=27.5$ eV Å^3.[25] Other typical parameters are electron density $n=2.4\times10^{15}$ m^{-2}, quantum well thickness $w=300$ Å, $l_e=1$ μm, and $l_{so}=2.9$ μm. The electrons occupy only the lowest subband in the quantum well. An electric field $E=25$ mV/μm is applied along x to set up the spin-Hall phenomenon.

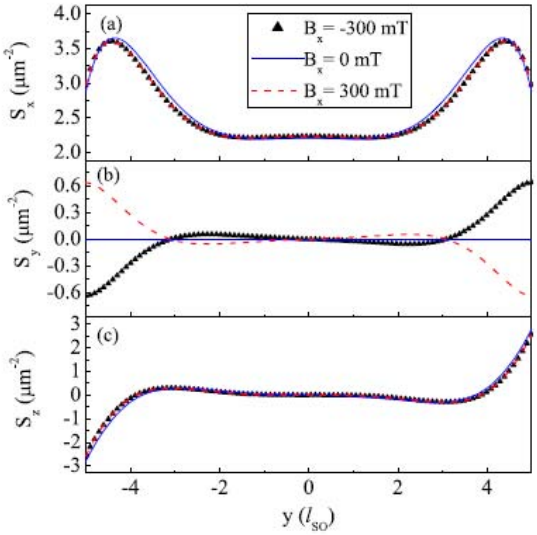

FIG. 2. (Color online) Spin densities S_i versus y, in units of l_{so}, for the case of a longitudinal in-plane magnetic field. Spin densities S_x, S_y, and S_z in units of μm^{-2} are shown in (a), (b), and (c), respectively, for magnetic fields $B_x=-300$ mT (black/ triangles), $B_x=0$ mT (blue/solid curve) and $B_x=300$ mT (red/dashed curve). The edges of the stripe are at $y=\pm5l_{so}$.

Longitudinal field orientation case is presented in Figs. 2(a)–2(c). Shown here are the spatial variations in all spin components of S_i across the stripe. S_x has both finite bulk spin density and edge spin accumulation. It exhibits even parity in its spatial variation and remains so for finite field B_x. The magnetic field causes only a minor change to the S_x profile while it has an even parity in its B_x dependence. S_y is zero at $B_x=0$ and has an edge spin accumulation in finite B_x. It is of odd parity in both its spatial and field dependencies. S_z has an edge spin accumulation. It is of odd and even parities in its spatial and field dependencies, respectively. Overall, except for S_y, the effects of B_x for the chosen range of field strengths is weak. That the spatial profile of S_y for finite fields mirrors that of S_z corroborates a spin precession picture as suggested by Eqs. (7). Following the $d\boldsymbol{\sigma}/dt = (2/\hbar)\tilde{\mathbf{B}}\times\boldsymbol{\sigma}$ time evolution, the precession of S_z contributes to S_y.

Transverse field orientation case is presented in Figs. 3(a) and 3(b). The field effects on the spin distributions and on the parity of the S_i profiles are much more dramatic. In short, the S_x and S_z profiles become asymmetric in both their spatial and field dependencies. S_y, however, remains zero in all these cases. Qualitative understanding of these changes can be obtained again from the spin precession picture. We take, for instance, the $B_x=-300$ mT curve for S_z in Fig. 3(b). The

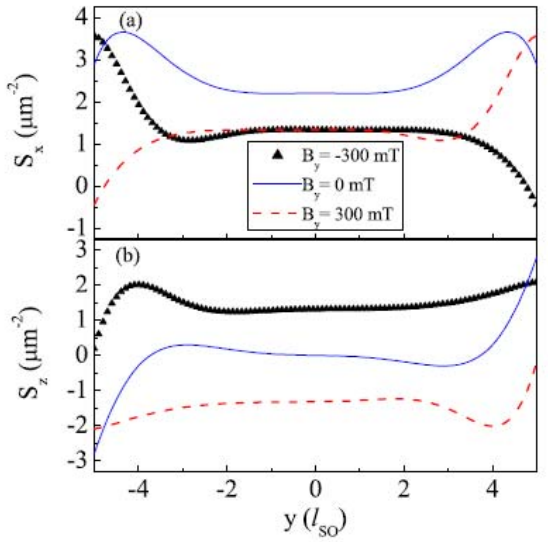

FIG. 3. (Color online) Spin densities S_i versus y for the case of a transverse in-plane magnetic field. Spin densities S_x and S_z in units of μm^{-2} are shown in (a) and (b), respectively, for magnetic fields $B_y=-300$ mT (black/triangles), $B_y=0$ mT (blue/solid curve), and $B_y=300$ mT (red/dashed curve). S_y remains zero in all these cases.

out-of-plane spin density $S_z \simeq 1.5$ μm^{-2} in the bulk is resulted from the precession of the zero-field S_x and also from a spin-charge coupling term in Eq. (8). On the other hand, the S_z edge spin accumulation is resulted from two spin precession processes, if we treat S_i as individual entities. First, the magnitude of S_z edge accumulation is reduced due to its own precession. However, it may be increased due to the precession of S_x. As the zero-field S_x is even and the zero-field S_z is odd in their spatial parity, it is inevitable that the magnitude of S_z will receive enhancement at one edge and suffer suppression at another. This leads to the breaking of the spatial parity of the S_z profile as is confirmed in Fig. 3. The zero-field S_i thus play a pivotal role in the shaping of the low in-plane magnetic-field S_i profile.

Figure 4 presents the edge spin accumulations of $S_i^{\pm}$ and their parity in their field dependencies. $S_i^{\pm}$ denote edge spin densities at $y=\mp d/2$. For the longitudinal field orientation depicted in Figs. 4(a) and 4(b), $S_x^{\pm}$ and $S_z^{\pm}$ are of even parity in B_x, whereas $S_y^{\pm}$ is of odd parity in B_x. The magnitude of the variation is comparable for $S_y^{\pm}$ and $S_z^{\pm}$, a feature consistent with our spin precession picture. More detailed symmetries can be read off from Eq. (7) and is given in the following: $S_{y(z)}^{+}=-S_{y(z)}^{-}$, $S_x^{+}=S_x^{-}$, $S_{x(z)}^{\pm}(B_x)=S_{x(z)}^{\pm}(-B_x)$, and $S_y^{\pm}(B_x)=-S_y^{\pm}(-B_x)$. For the transverse field orientation depicted in Figs. 4(c) and 4(d), $S_x^{\pm}$ and $S_z^{\pm}$ become asymmetric in their field dependencies, whereas $S_y^{\pm}=0$. The extremum points in $S_z^{\pm}$ at $B_y=50$ and -50 mT in Figs. 4(c) and 4(d), respectively, demonstrate the competition between the two spin precession processes: decreasing in magnitude due to its own precession and increasing in magnitude due to spin precession in $S_x^{\pm}$. Finally, if we include both the spatial and the

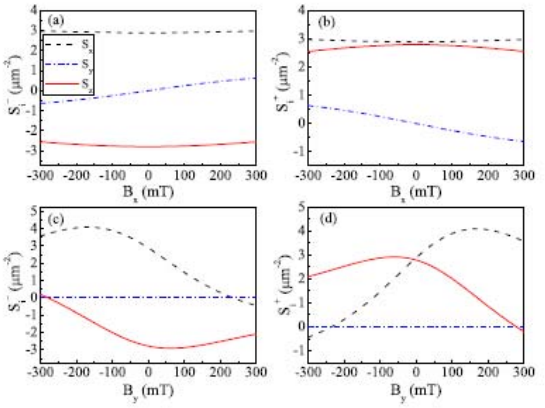

FIG. 4. (Color online) Edge spin densities $S_i^{\pm}$ versus magnetic field for both field orientations: longitudinal B_x cases in (a) and (b) and transverse B_y cases in (c) and (d). $S_i^{\pm}$ denotes spin densities at the edges $y=\mp d/2$. S_x is labeled by the dashed curve, S_y by the dashed-dotted curve, and S_z by the solid curve.

field reversals, we obtain symmetries $S_z^{+}(B_y)=-S_z^{-}(-B_y)$ and $S_x^{+}(B_y)=S_x^{-}(-B_y)$.

The entire spatial and field symmetries of the out-of-plane spin densities are presented in the contour plots in Fig. 5. In Fig. 5(a), the longitudinal field case exhibits even parity in B_x and odd parity in y. In contrast, the transverse field case, depicted in Fig. 5(b), exhibits much richer features. Even though the asymmetry of S_z with respect to B_y and y, individually, is evident, the symmetry $S_z(B_y,y)=-S_z(-B_y,-y)$ is also clearly shown. At the lateral edges, the highest spin densities are shifted from $B_y=0$. It is resulted from the two competing spin precession processes. Near the center of the sample, S_z is odd in B_y and its magnitude increases with the field as indicated in Eq. (8) already.

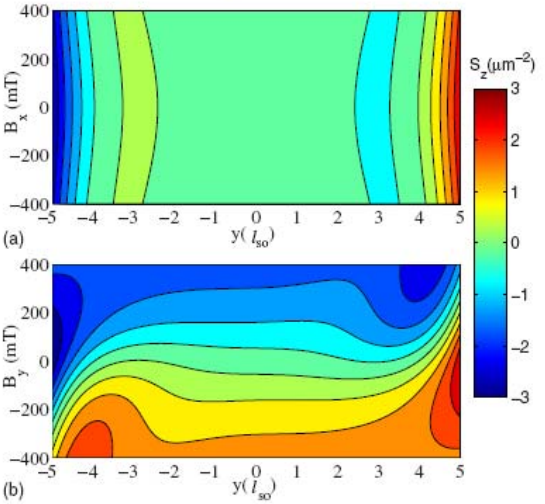

FIG. 5. (Color online) Contour plot of S_z on the B_i-y plane for (a) the longitudinal and (b) the transverse field orientations.

The strong in-plane magnetic-field anisotropy in the symmetry characteristics of the S_i profiles shown here is distinct for the Dresselhaus SOI. For the edge spin accumulation S_z in a transverse magnetic field, the Dresselhaus SOI leads to an asymmetric field dependence, whereas extrinsic SOI leads to a symmetric field dependence.[6] This symmetry characteristic for the extrinsic SOI is clearly seen in the experiment of Kato *et al.*[6] [Fig. 1(c) in Ref. 6], and also in their demonstration the S_z profile fits well to a Lorentzian function $A_0/[(\omega_L\tau_s)^2+1]$ which depends on even power of B through the square of the electron Larmor precession frequency ω_L. The factor A_0 is a proportionality constant and τ_s is the electron-spin lifetime. As for the Rashba SOI, symmetry governs that we turn to longitudinal magnetic field. We find no S_z both in the bulk and at edges, which is consistent with previous finding.[11] In contrast, we find that the Dresselhaus SOI leads to an even-parity field dependence. Nonvanishing bulk spin density S_z due to Rashba SOI, but for the case of either anisotropic scatterers or nonparabolic electron dispersion, has been obtained by Engel *et al.*[11] and the field dependence is of odd parity.[11,17] Thus we commence the notion of utilizing low in-plane magnetic field for the determination of the underlying SOI in a particular sample, without the need to prepare controlling samples of different crystal orientations.

IV. CONCLUSION

In conclusion, we have performed a systematic and comprehensive study on the effects of a weak in-plane magnetic field on the bulk spin densities and edge spin accumulations in a diffusive Dresselhaus-type 2D stripe. Our results show that out-of-plane spin density can be generated in the case of transverse field orientation without assuming anisotropic scatterers or nonparabolic electron dispersion relations. The breaking of the parity of the spin distributions with respect to their spatial and field dependencies provide a unique signature for the Dresselhaus SOI. This work thus points to the possibility of invoking weak in-plane magnetic fields for the determination of the SOI in a particular sample.

ACKNOWLEDGMENTS

This work was supported by Taiwan NSC (Contract No. 96-2112-M-009-0038-MY3), NCTS Taiwan, Russian RFBR (Contract No. 060216699), and a MOE-ATU grant. We are grateful to the Centre for Advanced Study in Oslo for hospitality.

[1] M. I. Dyakonov and V. I. Perel, Phys. Lett. **35A**, 459 (1971).
[2] V. M. Edelstein, Solid State Commun. **73**, 233 (1990).
[3] J. E. Hirsch, Phys. Rev. Lett. **83**, 1834 (1999).
[4] S. Murakami, N. Nagaosa, and S. C. Zhang, Science **301**, 1348 (2003).
[5] J. Sinova, D. Culcer, Q. Niu, N. A. Sinitsyn, T. Jungwirth, and A. H. MacDonald, Phys. Rev. Lett. **92**, 126603 (2004).
[6] Y. K. Kato, R. C. Myers, A. C. Gossard, and D. D. Awschalom, Science **306**, 1910 (2004).
[7] J. Wunderlich, B. Kaestner, J. Sinova, and T. Jungwirth, Phys. Rev. Lett. **94**, 047204 (2005).
[8] S. Q. Shen, Phys. Rev. B **70**, 081311(R) (2004).
[9] E. I. Rashba, Sov. Phys. Solid State **2**, 1109 (1960); Yu. A. Bychkov and E. I. Rashba, JETP Lett. **39**, 78 (1984).
[10] H. A. Engel, B. I. Halperin, and E. I. Rashba, Phys. Rev. Lett. **95**, 166605 (2005).
[11] H. A. Engel, E. I. Rashba, and B. I. Halperin, Phys. Rev. Lett. **98**, 036602 (2007).
[12] G. Dresselhaus, Phys. Rev. **100**, 580 (1955).
[13] A. G. Mal'shukov and K. A. Chao, Phys. Rev. B **71**, 121308(R) (2005).
[14] W. K. Tse and S. DasSarma, Phys. Rev. B **74**, 245309 (2006).
[15] J. I. Inoue, G. E. W. Bauer, and L. W. Molenkamp, Phys. Rev. B **70**, 041303(R) (2004); E. G. Mishchenko, A. V. Shytov, and B. I. Halperin, Phys. Rev. Lett. **93**, 226602 (2004); A. A. Burkov, A. S. Núñez, and A. H. MacDonald, Phys. Rev. B **70**, 155308 (2004); R. Raimondi and P. Schwab, *ibid.* **71**, 033311 (2005); O. V. Dimitrova, *ibid.* **71**, 245327 (2005); B. A. Bernevig and S. C. Zhang, Phys. Rev. Lett. **95**, 016801 (2005).
[16] A. G. Mal'shukov, L. Y. Wang, C. S. Chu, and K. A. Chao, Phys. Rev. Lett. **95**, 146601 (2005).
[17] Y. K. Kato, R. C. Myers, A. C. Gossard, and D. D. Awschalom, Phys. Rev. Lett. **93**, 176601 (2004).
[18] N. P. Stern, S. Ghosh, G. Xiang, M. Zhu, N. Samarth, and D. D. Awschalom, Phys. Rev. Lett. **97**, 126603 (2006).
[19] H. A. Engel, Phys. Rev. B **77**, 125302 (2008).
[20] R. V. Shchelushkin and A. Brataas, Phys. Rev. B **72**, 073110 (2005).
[21] Q. Lin, S. Y. Liu, and X. L. Lei, Appl. Phys. Lett. **88**, 122105 (2006).
[22] P. Lucignano, R. Raimondi, and A. Tagliacozzo, Phys. Rev. B **78**, 035336 (2008).
[23] M. Milletarì, R. Raimondi, and P. Schwab, Europhys. Lett. **82**, 67005 (2008).
[24] A. A. Abrikosov, L. P. Gorkov, and I. E. Dzyaloshinskii, *Method of Quantum Field Theory in Statistical Physics* (Dover, New York, 1975).
[25] *Spin-Orbit Coupling Effects in Two-Dimensional Electron and Hole Systems*, edited by Roland Winkler (Springer-Verlag, Berlin, 2003).
[26] O. Bleibaum, Phys. Rev. B **74**, 113309 (2006).
[27] Y. Tserkovnyak, B. I. Halperin, A. A. Kovalev, and A. Brataas, Phys. Rev. B **76**, 085319 (2007).
[28] J. R. Shi, P. Zhang, D. Xiao, and Q. Niu, Phys. Rev. Lett. **96**, 076604 (2006).
[29] P. Zhang, Z. G. Wang, J. R. Shi, D. Xiao, and Q. Niu, Phys. Rev. B **77**, 075304 (2008).
[30] V. Sih, W. H. Lau, R. C. Myers, V. R. Horowitz, A. C. Gossard, and D. D. Awschalom, Phys. Rev. Lett. **97**, 096605 (2006).